

Review

# The Breaking of Symmetry Leads to Chirality in Cucurbituril-Type Hosts

Riina Aav \*  and Kamini A. Mishra 

Department of Chemistry and Biotechnology, School of Science, Tallinn University of Technology, Akadeemia tee 15, 12618 Tallinn, Estonia; kamish@ttu.ee

\* Correspondence: riina.aav@ttu.ee; Tel.: +372-620-4365

Received: 2 February 2018; Accepted: 30 March 2018; Published: 5 April 2018



**Abstract:** Cucurbituril-type hosts are highly symmetric, but there are means to break their symmetry. This review will present examples from three directions of induction of chirality in or by cucurbituril-type hosts: first, through the incorporation of stereogenic elements into host molecules; second, through complexation with achiral guests, which leads to axial supramolecular chirality and helical structures; third, through the formation of complexes with chiral guests in multi-molecule complexes and induction of supramolecular chirality. In addition, a list of chiral guests used in binding studies with cucurbiturils is collected. We would envision that encouraged by the outlined examples of outstanding applications of chiral cucurbituril-supramolecular systems, the boundaries of chiral applications of cucurbiturils would be widened.

**Keywords:** cucurbiturils; hemicucurbiturils; chirality; supramolecular chirality; symmetry breaking; helices

## 1. Introduction

Cucurbituril (CB)-type hosts are oligomeric compounds, where cyclic urea monomers are connected through methylene bridges. Core CBs are double-bridged macrocycles, which are made from glycoluril and formaldehyde [1–4]. Further on, the family has enlarged [5–7]. One can divide CBs into two main branches: the double-bridged and single-bridged CBs (Figure 1). All CBs have hydrophobic cavities, but electronic binding properties are different for single- and double-bridged CBs. Double-bridged CBs bind cations at the portals and single-bridged CBs anions in their cavity. All single-bridged CBs can be viewed as derivatives of hemicucurbiturils (HCs). HCs are formed in condensation of ethylene urea and formaldehyde, and cyclohexano-HC, bambusurils and biotinuril all contain linked ethylene urea moieties in their structures.

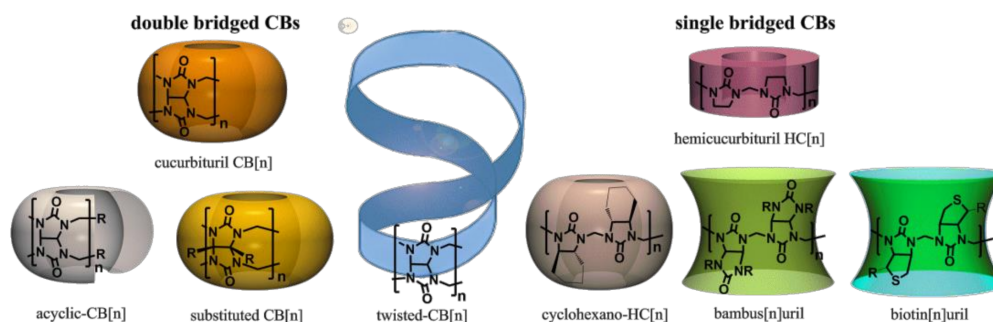


**Figure 1.** Cucurbituril-type hosts. CB, cucurbituril; HC, hemicucurbituril.

CB chemistry has been reviewed from various aspects [5–28], though so far, only one focused on the chirality of CBs [29]. CB-type hosts are very symmetric, but there are means to break this symmetry. This review will present examples from three directions of inducing chirality in CB chemistry: first, through the incorporation of stereogenic elements into the structure of CBs, through stereogenic atoms and helices; second, through complexation with achiral guests, which leads to axial supramolecular chirality in the helical structures; third, through the formation of complexes with chiral guests in multi-molecule complexes and induction of supramolecular chirality. In addition, a list of chiral guests that have been used in studies with CB-type hosts is collected.

## 2. Chiral Cucurbituril-Type Hosts

In general, the structures of core cucurbiturils are very symmetric. The CB[6] has seven planes of symmetry, as shown in Figure 2. Three vertical planes of symmetry pass through urea oxygens and three vertical planes through methylene bridges; additionally, one horizontal plane goes through the equator of the macrocycle.

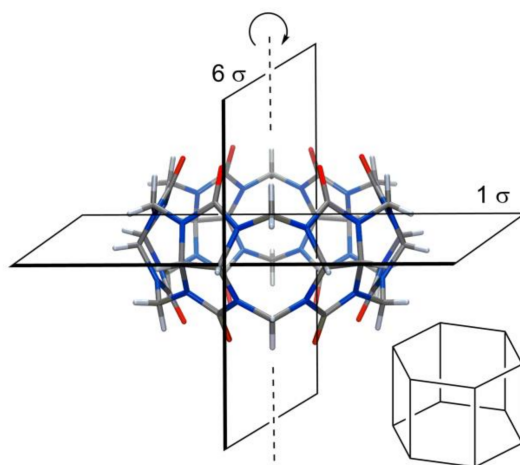
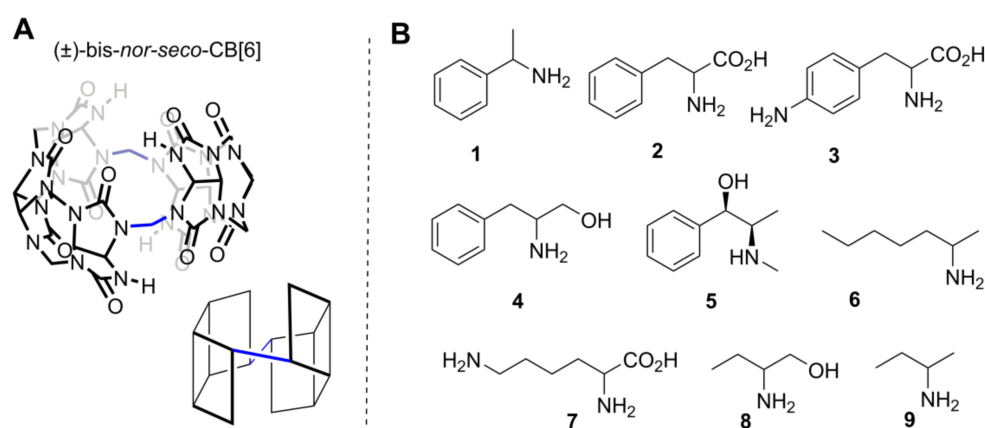


Figure 2. CB[6] and its planes of symmetry.

Because of these symmetry planes, neither substitution at a single methylene bridge nor at hydrogens of monomers by achiral groups will lead to chirality in the CB. To induce chirality, one must make changes at least at two methylene bridges in a way that disrupts all symmetry planes. In ( $\pm$ )-bis-*nor-seco*-CB[6] (Figure 3A), two methylene bridges are missing and trimeric glycolurils are connected in a diagonal fashion. Because of this, all glycoluril CH carbons become stereogenic, and as there are no symmetry planes, the macrocycle is chiral. Of course, if such a compound is formed in an achiral medium, then equal amounts of enantiomers are produced [30].

Isaacs et al. investigated the formation of host–guest complexes of ( $\pm$ )-bis-*nor-seco*-CB[6] in D<sub>2</sub>O with a number of chiral compounds (Figure 3B) [30]. Intriguingly, differences in NMR signals were noted while complexes were formed from enantiopure or racemic guests with ( $\pm$ )-bis-*nor-seco*-CB. This observation is clear evidence of the formation of different supramolecular complexes. In a simple system, when one host enantiomer forms a complex with an enantiomerically pure guest, a single enantiomerically pure complex is formed. If an enantiomerically pure guest complexes with the chiral racemic host, then a mixture of two diastereomeric and enantiomerically pure complexes will be formed. By <sup>1</sup>H-NMR spectroscopy, one can distinguish diastereomers, and therefore, two sets of signals can appear. Now, if both chiral compounds would be mixed as racemates, then the same two diastereomeric complexes will be formed, just racemic complexes. By a simple NMR measurement, one cannot see the difference between enantiomerically pure and racemic complexes; therefore, the NMR spectra are expected to be the same. The situation with ( $\pm$ )-bis-*nor-seco*-CB[6] is not that simple. Isaacs et al. noted that the ratio of diastereomeric host–guest complexes is influenced by the guest stereoisomeric

purity. The reasons for these observations were not disclosed, but the aggregation of one or both chiral entities used in the study might have influenced the NMR signals [31,32]. Binding dynamics were dependent on the structure of the guest, as NMR spectra of ( $\pm$ )-bis-*nor-seco*-CB[6] showed increased complexity and multiplicity in the presence of an aromatic chiral guest, referring to binding where guests are not exchanged on the NMR timescale. On the other hand, NMR peaks became very broad upon complexation with aliphatic guests, referring to association-dissociation during the measurement at room temperature.



**Figure 3.** (A) One enantiomer of ( $\pm$ )-bis-*nor-seco*-CB[6]; (B) chiral guest whose binding was studied with ( $\pm$ )-bis-*nor-seco*-CB[6].

According to our knowledge, only a few chiral compounds have been isolated to date from the condensation reaction between glycoluril and formaldehyde, the abovementioned ( $\pm$ )-bis-*nor-seco*-CB[6] and acyclic 10-membered oligomer [33] (Figure 4), which have stereogenic atoms and twisted-CBs [34–36], which possess axial chirality (Figure 6). In the acyclic 10-membered oligomer, two pentamers are connected to each other through a single bond with no plane of symmetry.

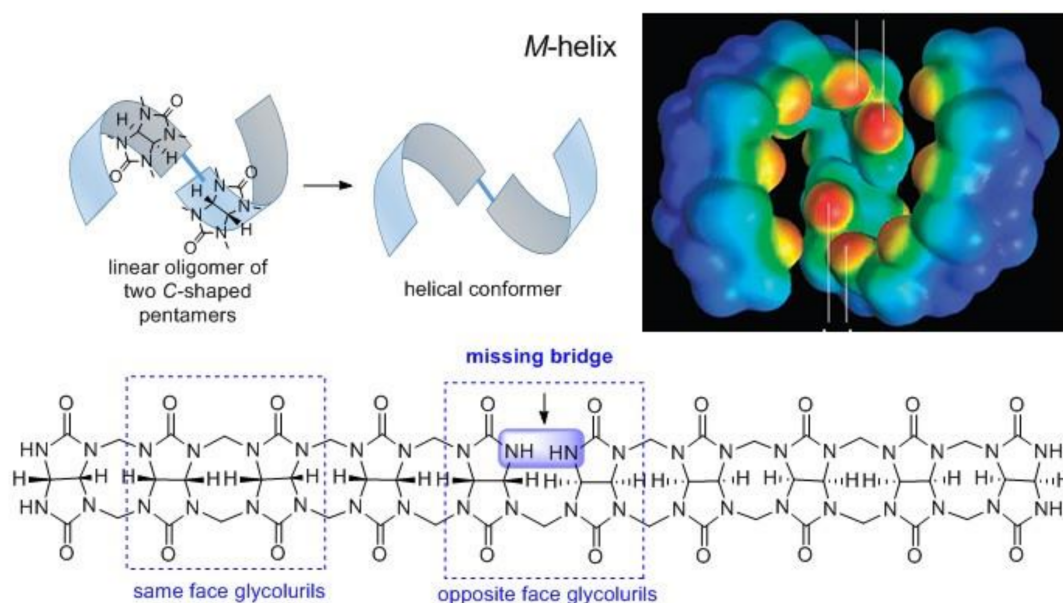


**Figure 4.** Map of electronic potential of a single enantiomer of the ( $\pm$ )-glycoluril decamer in the shape of an *M*-helix (adopted with permission from [33]) and its structure.

It is remarkable how a very small change in the structure of the oligomer, like the single turn of the face of the glycoluril and disconnection of one methylene bridge, can affect the geometry of the molecule. Oligomers, where same face glycolurils are linked, have a C-letter-shaped conformation, and they are achiral and can form a macrocycle. Absence of one methylene bridge in ( $\pm$ )-glycoluril decamer turns all glycoluril CH carbon atoms stereogenic, which induced its crystallization in a helical conformation. As this compound was formed in an achiral medium, two opposite-handed helixes were formed in a ratio of 1:1 [33]. Binding with chiral guests was not probed with ( $\pm$ )-glycoluril decamer.

C-letter-shaped conformation of glycoluril oligomers and their ability to bind guest through electrostatic interactions with glycoluril carbonyl groups encouraged Isaacs to develop a new branch type of CB-type molecules, the acyclic CBs. To enrich oligomer structure with sites for additional functionalization and to add UV-active properties, Isaacs used substituted aromatic groups at the terminus of acyclic CBs. The structures of chiral and enantiopure acyclic CBs are shown in Figure 5A [37].

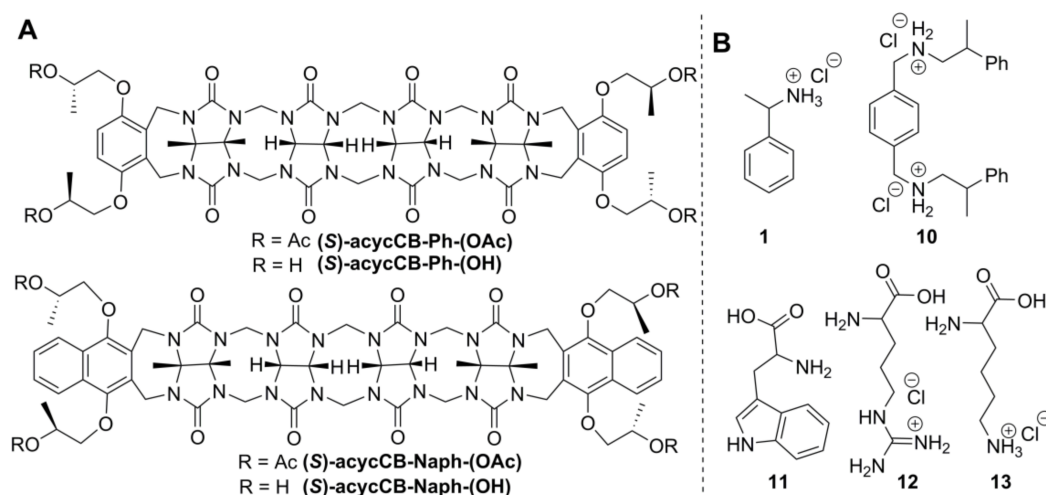


**Figure 5.** (A) Chiral acyclic CBs; (B) chiral guests, whose binding was studied with acyclic CBs [37].

Chiral acyclic CBs showed binding with ammonium-functionalized guest (Figure 5B) in acetic acid buffer at pH 5.5, and association constants were found to be in range of  $10^3$ – $10^6$  M<sup>-1</sup>. Small enantioselectivity in the binding of opposite enantiomers was also detected. The ratio of association constants for binding the (*S*)-1 over (*R*)-1 the  $K_{(S)}/K_{(R)}$  was 1.3 for binding with (*S*)-acycCB-Ph-(OAc). Unfortunately, the binding of guest 1 to host (*S*)-acycCB-Ph-(OH) and guest 10 to both chiral acyclic CBs (*S*)-acycCB-Ph-(OAc) and (*S*)-acycCB-Ph-(OH) gave very close  $K_{(S)}$  and  $K_{(R)}$  values, and as the differences in measured  $K$  values were in the range of the measurement uncertainty, one can conclude that enantiodiscrimination is either absent or very small. The hosts (*S*)-acycCB-Naph-(OAc) and (*S*)-acycCB-Naph-(OH) were also able to bind cationic guests, but association constants could not be determined.

Isaacs has also developed a synthesis of functionalized CBs through macrocyclization of glycoluril hexamer and substituted glycoluril. By this strategy, amino acids and biotin were linked covalently to CBs, and efficient uptake of Oxaliplatin by cancer cells was achieved [38]. Recently, a polymeric biomaterial was prepared from glucose-based polymer: dextran and covalently-bound acyclic CB. This sugar-based chiral polymer was used for encapsulation of antitumor drugs, and its chiral properties were not investigated [39].

Apart from the listed CBs, which incorporate stereogenic centers in their structure, there is a special sub-class of CBs, which do not have stereocenters, but are still chiral. These are twisted CBs with axial chirality. The crystal structure of CB[14] revealed helical conformations of this CB, and therefore, the name *twisted*-CB[14] [34,35] was given (Figure 6). Currently there are three known CBs with 13,

14 and 15 glycolurils in their structures that have a helical conformation (Figure 6). Twisted CBs have a  $360^\circ$  turn in their oligomer belt, and the direction of this turn defines the stereochemistry of the macrocycle. Helical conformation is locked into the macrocyclic structure. One should mention that, in *twisted*-CB[13–15]s [34,36], the belt is formed so that all glycoluril monomers have the same faces linked next to each other, so these are not Möbius band [40]. Curiously, in aqueous solution, without any guests, *twisted*-CB[14] looks like normal cucurbituril, having only three signals in its  $^1\text{H-NMR}$ . Despite that, complexation studies of *twisted*-CB[14] in solution showed binding of a 1,8-octyldiammonium in a 1:1 stoichiometry, similarly to CB[8], with a  $K_a$  of  $7.9 \times 10^6 \text{ M}^{-1}$ , and smaller 1,4-butyldiammonium guest binds in a 1:2 ratio, with  $K_a$  values of  $1.9 \times 10^8 \text{ M}^{-1}$  and  $2.9 \times 10^6 \text{ M}^{-1}$ , indicating clearly that *twisted*-CB[14] has two separate binding compartments and that these compartments are adaptable [41].

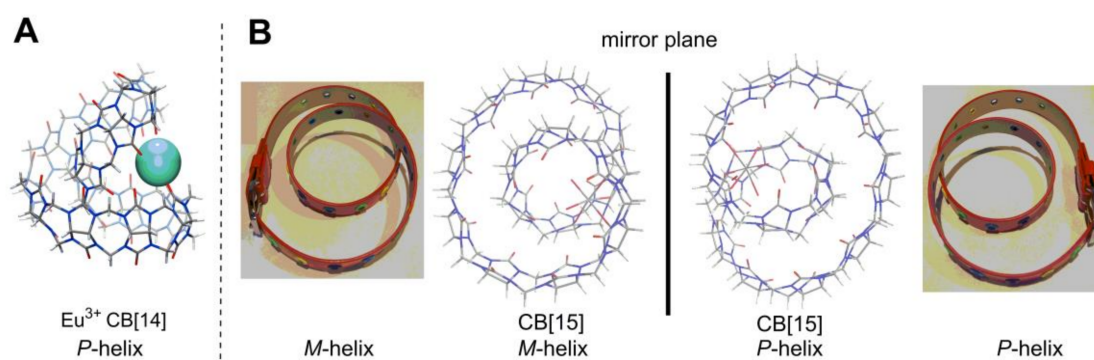


**Figure 6.** (A) ( $\text{Eu}^{3+}$ ·CB[14]) side view of *P*-helix [34]; (B) top view of ( $\text{Cd}^{2+}$ ·CB[15]) in *M*- and *P*-helical conformations formed in the same crystal [36] and illustration of these helix configurations with a belt.

Single-bridged CB-type macrocycles (Figure 1), the hemicucurbiturils [6,42] (HC), also have high symmetry like most CBs. The structure of an unsubstituted six-membered HC is shown in Figure 7. The monomers of HC are positioned in a “zig-zag” manner; therefore, HCs have fewer planes of symmetry in their structure than the parent CBs. Six-membered unsubstituted HC (Figure 7) and substituted HCs, which are formed from achiral monomers (Figure 8A), have three planes of symmetry.

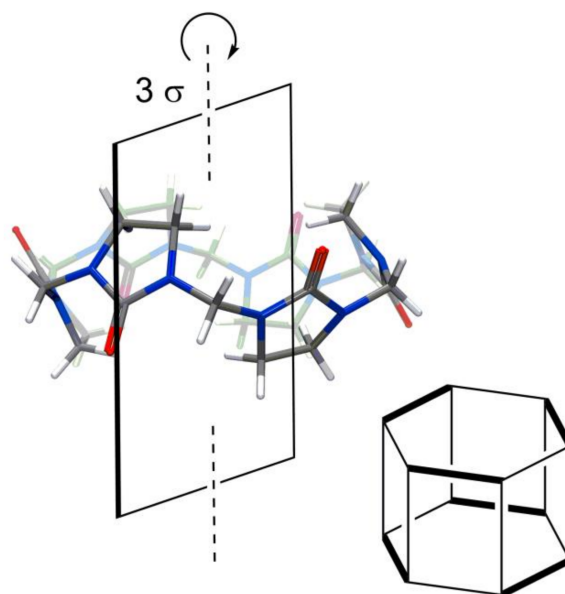


**Figure 7.** Hemicucurbit[6]uril [42] and its planes of symmetry.

Bambusurils [22,43] are a sub-class of single-bridged CBs that are made of achiral monomers (Figure 8B). One can see that nonequivalent R-substituents at glycolurils would lead to desymmetrization and creation of stereogenic centers at carbons of fused cycles. In this way, the formation of chiral bambusurils would be feasible.

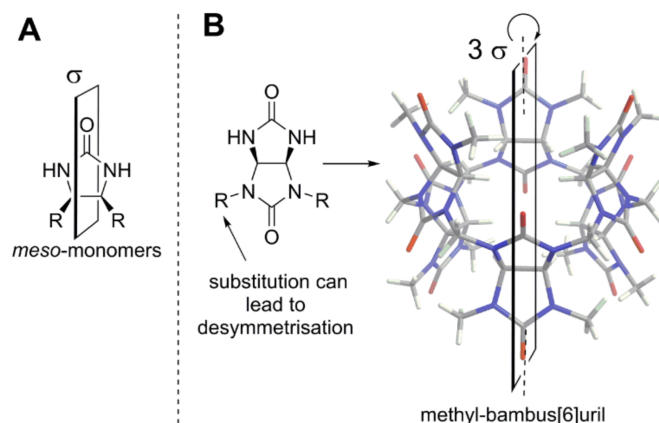


**Figure 8.** (A) The general structure of achiral substituted ethylene urea; (B) crystal structure of achiral methyl-bambus[6]uril [43] and its monomer.

Very interesting desymmetrization was achieved in azabambusuril [23,44] (Figure 9): substitution of a sulfur atom in symmetric thiobambusurils with an alkylimine moiety leads to the loss of all symmetry planes in this macrocycle.

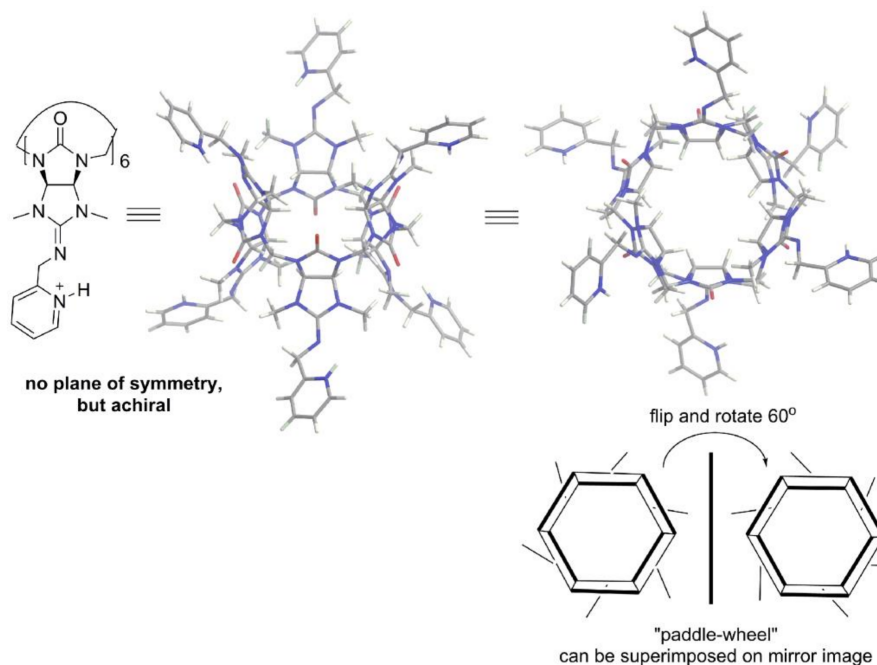


**Figure 9.** Drawing and crystal structure of protonated picolyl-azabambusuril [44] and cartoon of its “paddle-wheel” configuration.

The alkyl-azabambusuril crystal structure [44] revealed its “paddle-wheel”-like configuration. The unidirectional orientation of the imine double bonds in azabambusuril (Figure 9, right side), reflects high diastereoselectivity during their formation. Curiously, in spite of the desymmetrization

of bambusuril monomer, alkyl-azabambusuril is achiral, as its mirror image can be superimposed by flipping and rotating this “paddle-wheel” (Figure 9). Nevertheless, in the future chiral bambusurils could be made from nonuniformly substituted monomers.

As one can see, HCs have many options for the incorporation of stereogenic atoms into their structure, and several of them have been prepared in enantiopure form with high yield and in a single macrocyclization step [45–47]. Chiral (*S,S*)- or (*R,R*)-cyclohexano-hemicucurbit[6,8]urils (cycHC) are derived from enantiopure cyclohexa-1,2-diylurea [45,47] (Figure 10A), and biotin[6]uril from the vitamin biotin [46] (Figure 11).

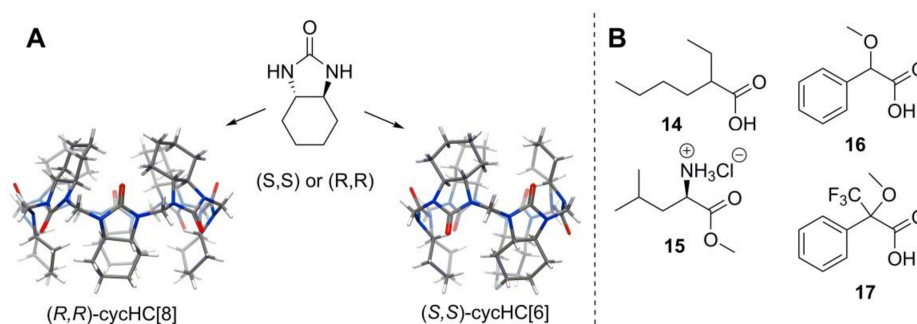


**Figure 10.** (A) Structure of cyclohexa-1,2-diylurea and crystal structure of chiral cycHCs [45,47]; (B) chiral guests whose binding was studied with cycHCs [47].

Enantiopure (*S,S*)-cycHC[6] binding ability has been tested on some chiral compounds shown in Figure 10B. Association constants determined by DOSY NMR in  $\text{CDCl}_3$  were quite low and remained in the range  $10^1$ – $10^2 \text{ M}^{-1}$ . The (*R,R*)-cycHC[6] [45] showed a preference for binding of (*R*)-**16** and (*R,R*)-cycHC[8] [47] for (*S*)-**16**, with a  $K_{(R)}/K_{(S)}$  value of 1.4 and  $K_{(S)}/K_{(R)}$  of 2.0, respectively. Interestingly, the guest **17**, whose acidity and also association constant was higher than those of **16**, bound to (*R,R*)-cycHC[8] nonstereoselectively. No crystal structures of these complexes were obtained; therefore, the position of the guests is not fully disclosed.

Nevertheless, a tentative binding mode of guests to cycHCs was proposed based on ion-mobility MS of cycHC[6] complexes with  $\text{Na}^+$  and anions, accompanied by DFT calculations of neutral molecules and anions [48]. Anions form inclusion complexes with cycHCs, and undissociated carboxylic acids form external complexes through hydrogen bonding with the urea carbonyl group. (Figure 11A).

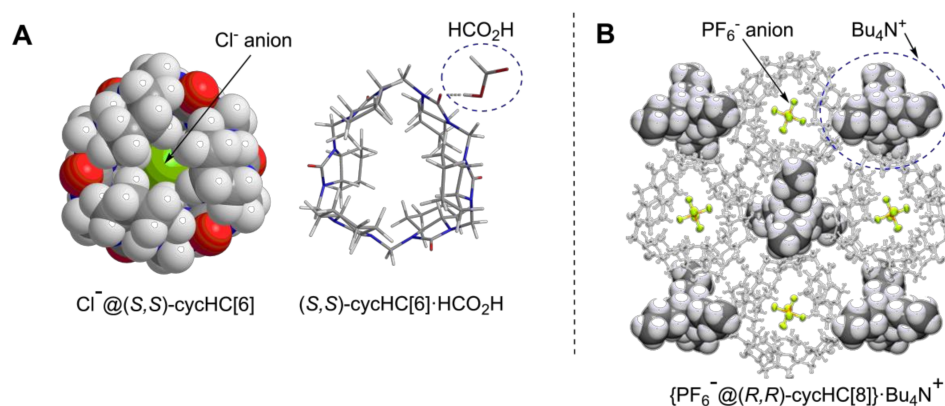


**Figure 11.** (A) Minimum energy geometry of inclusion complex of  $\text{Cl}^- @(\text{S,S})\text{-cycHC[6]}$  and external complex of  $(\text{S,S})\text{-cycHC[6]}\cdot\text{HCO}_2\text{H}$  [48]; (B) crystal structure of  $(\text{PF}_6^- @(\text{R,R})\text{-cycHC[8]})\cdot\text{Bu}_4\text{N}^+$  [49], Published by The Royal Society of Chemistry.

The crystal structure of the tetrabutylammonium hexafluorophosphate complex with (*R,R*)-cycHC[8] (Figure 11B) [49] confirmed the previous hypotheses that an anion can be encapsulated and that the cation forms an external complex with this host.

Another enantiopure member of single-bridged CBs is biotin[6]uril [46] (Figure 12), but so far, only its binding to achiral anions has been studied [50,51], and no reports on its stereoselective applications have been presented yet.

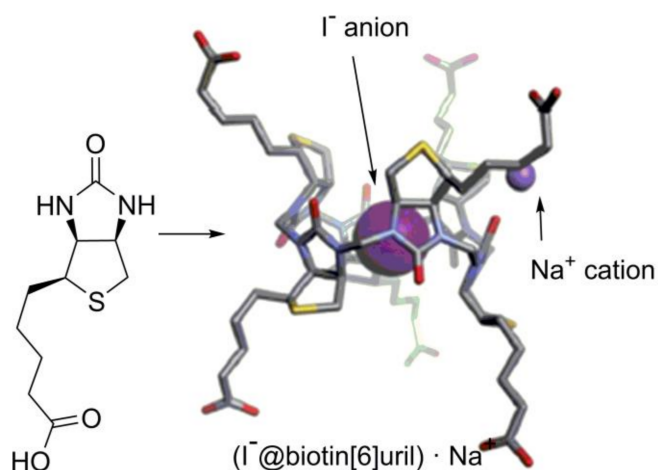


**Figure 12.** Biotin structure and crystal structure of the  $(\text{I}^- @ \text{biotin}[6] \text{uril}) \cdot \text{Na}^+$  complex [46].

Noteworthy is the diastereoselectivity of biotin[6]uril formation. Biotin is the most unsymmetrical urea monomer that has been used for making CB-type macrocycles. It does not have any symmetry elements in its structure, and therefore, the possibility of the formation of nine diastereomeric six-membered HCs exists. In spite of that, only a single diastereomer was formed during biotin condensation with formaldehyde [46]. This is the result of the dynamic formation of methylene bridges, which drives equilibrium toward the formation of the thermodynamically most favorable macrocycle.

From the examples above, one can see that several chiral hosts are known in the CB family, though their chiral recognition properties are barely studied, and their applications are awaiting.

### 3. Breaking Symmetry through Complex Formation with Achiral Compounds

The symmetry of achiral CBs might also be broken through complexation. The majority of studies in the field of CB chemistry are associated with binding affinity and their applications. Here, just some references to reviews are given [24,25]. Depending on the application, different non-covalent interactions become important. In the solid state [26,27,52], some examples exist, where achiral ligands can cause spontaneous resolution during crystallization and right- or left-handed chiral crystals are produced with equal probability. Examples where chiral helices have been formed with CB complexes are presented in this section.

The first helical structure formed upon complexation of the achiral ligand with CB was reported by Kim et al. [53]. A helix was constructed based on ammonium cation-dipole interaction between a guest and CB and silver cation-dipole interaction between pseudorotaxanes. A polyrotaxane chain was formed from CB[6], *N,N'*-bis(3-pyridylmethyl)-1,5-diaminopentane and  $\text{AgNO}_3$ . The crystal structure had an equal number of right- and left-handed helices, so it was racemic. (Figure 13, on the left). Later, along with several achiral polyrotaxanes, another helical racemic polyrotaxane was reported by Kim's group [54]. In that, a silver ion was exchanged with a cadmium ion, and as a result, a longer helical pitch was formed (Figure 13, on the right).

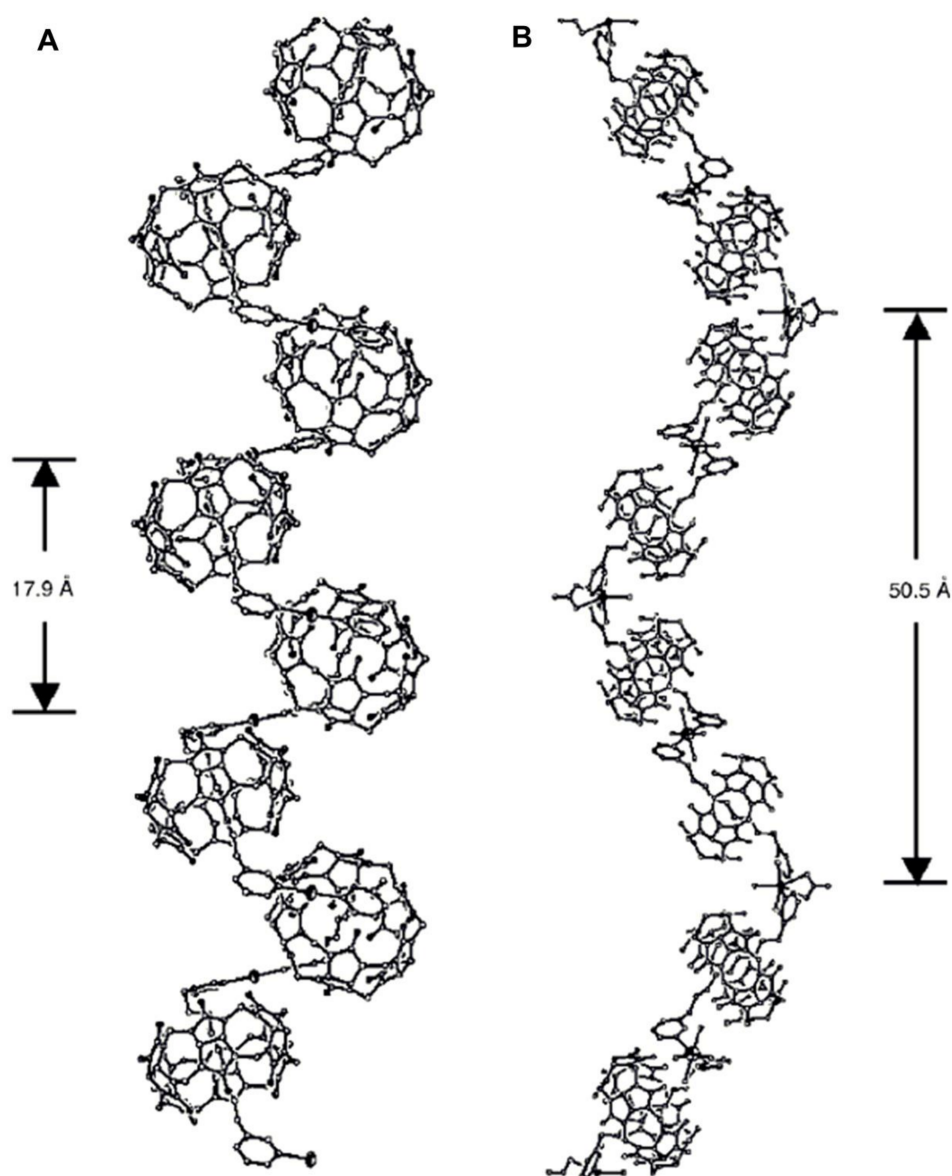


**Figure 13.** CB[6] polyrotaxane formed from CB[6] (A) *N,N'*-bis(3-pyridylmethyl)-1,5-diaminopentane and  $\text{AgNO}_3$  [53] (B) or  $\text{Cd}(\text{NO}_3)_2$  [54]; reproduced from [54].

Solid phase complexes with both handed helical networks of polyrotaxane were also shown by Xue and Liu et al., upon complex formation from *N,N'*-bis(2-pyridylmethyl)-1,6-hexanediamine, tetramethyl-CB[6] and  $\text{AgNO}_3$ . In the reported structure, CBs are aligned, as the dumbbell of rotaxane, which is constructed from substituted hexanediamine, taking a helical conformation. The authors state that the source of conformational chirality is the linkage of two 2-pyridylmethyl moieties with the silver ion [55].

Helical solid-state structures might be constructed also without pseudorotaxane formation. The network of CBs in Figure 14 is built through cation-dipole interaction and halogen bonding. CB[6] sodium cationic units are connected with copper(II) anionic complexes, the  $[\text{Cu}(\text{3,5-diiodosalicylate})(\text{8-hydroxyquinoline-5-sulfonate})]^{2-}$  [56] (Figure 14A). Right- and left-handed helices were both incorporated into a racemic crystal structure. Further, Chen, Liu, Yamauchi et al. [56] noted that upon exchange of iodo-ligand  $[\text{Cu}(\text{3-iodobenzoate})(\text{8-hydroxyquinoline-5-sulfonate})\text{Cl}]^{2-}$  was formed, which had all CB-chains organized into homochiral helix (Figure 14B).

The research group of Tao and Liu [57] reported the formation of a pair of homochiral 1-D-helical coordination polymers of CB[5] with  $\text{Dy}^{3+}$  upon crystallization in the presence of achiral hydroquinone (Figure 15). The interaction between hydroquinone and CB through  $\pi$ -H-C and  $\pi$ - $\pi$  stacking might direct the formation of a chiral helix.

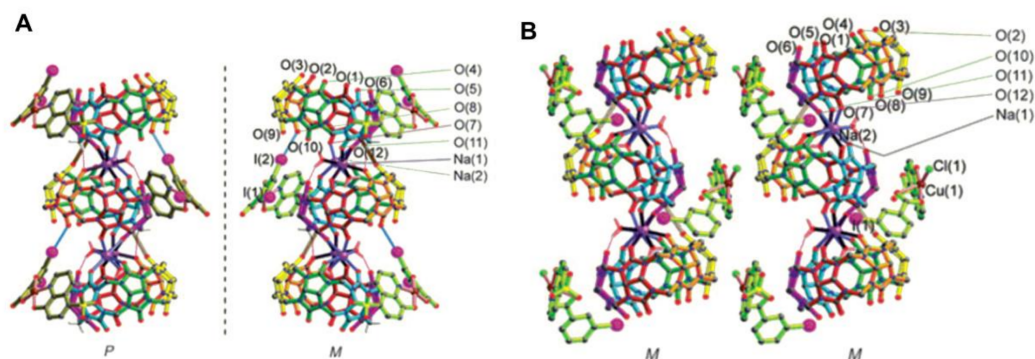


**Figure 14.** (A) Racemic  $[\text{CB}[6]\text{Na}_2\cdot\text{Cu}(3,5\text{-diiodosalicylate})(8\text{-hydroxyquinoline-5-sulfonate})]$ ; (B) homochiral  $[\text{CB}[6]\text{Na}_2\cdot\text{Cu}(3\text{-iodobenzoate})(8\text{-hydroxyquinoline-5-sulfonate})\text{Cl}]$ . Reproduced from [56].

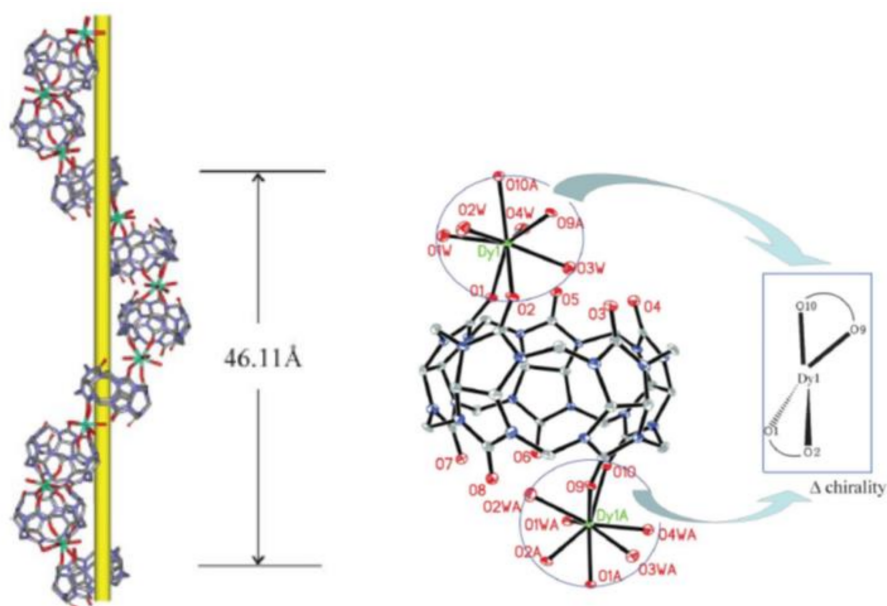


**Figure 15.** Right-handed *P*-helix and network structure of  $(\text{CB}[5]\text{Dy}(\text{H}_2\text{O})_4\text{CB}[5])^{3+}$  and hydroquinone, crystallized in space group  $P6_1$  [57], reproduced from [57] with permission from The Royal Society of Chemistry.

In the crystal structure with a *P*-helix, two carbonyl groups of CB[5] are coordinated to  $\text{Dy}^{3+}$  and as every  $\text{Dy}^{3+}$  is connected with two CB[5] molecules; also,  $\text{Dy}^{3+}$  is chiral and has the  $\Delta$ -configuration. The authors attempted also a measurement of circular dichroism (CD) of single crystal, but unfortunately could not detect a reliable CD signal. The absolute configuration was assigned by single crystal diffraction analysis through the Flack parameter. Intriguingly, randomly performed crystallizations showed that two clusters crystallized in the space group  $P6_5$ , whereas the other six clusters crystallized in the space group  $P6_1$ . In other words, the sample in the present case had undergone spontaneous resolution with an enantiomeric excess value of 50% [57]. Formation

of similar helical networks has also been observed with heavy lanthanides like  $\text{Er}^{3+}$ ,  $\text{Yb}^{3+}$  or  $\text{Lu}^{3+}$ , but not with light lanthanides [58].

The given examples of helical polyrotaxanes show that upon understanding the supramolecular interactions of CBs with guests and with the suitable interplay between participating species, one can obtain chiral material. On the other hand, helical networks with CBs are relatively rare, compared with solid-state structures of coordination polymers made by the incorporation of various CBs. Therefore, one could state that induction of chirality in the solid state with CBs has been the result of good luck, and further research is required to develop an understanding for directed design.

In addition to the formation of helices from CB units, one can utilize larger homologues of CBs as a confined space, in which the helix can be fitted. Tao et al. [59] have shown that CB[8] is large enough to fold a long-hydrocarbon guest into a helix conformation within its cavity (Figure 16). The asymmetric unit of CB[8] pseudorotaxanes contained both the right- and left-handed helical guests in equal occupancy in its structure.

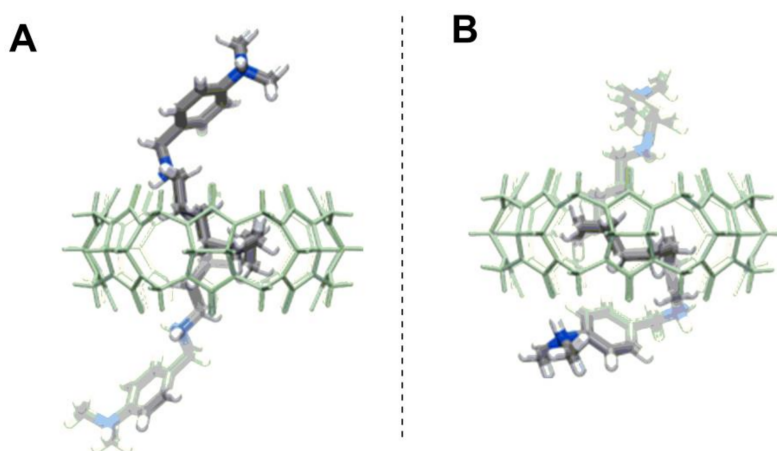


**Figure 16.** *N,N'*-bis(4-dimethylaminobenzyl)-dodecane-1,12-diamine folded inside of the CB[8] (A) into a right-handed helix; (B) into a left-handed helix [59].

One can see that CBs can be involved in the formation of chiral helical structures, but so far, stereoselectivity of this process has not been directed. Hopefully, future methods for homochiral and stereoselective helix formation will be developed, for example through seeding or by some chiral stimulus.

#### 4. Breaking Symmetry through Complex Formation with Chiral Compounds

It is clear that upon complexation with an enantiomerically pure guest, the entire host-guest complex becomes chiral. The situation becomes more intriguing if such a supramolecular complex can be applied in further chirogenesis or enantiodiscrimination [60,61].

One of the most reliable methods to detect chirality is CD. Cucurbiturils' carbonyl-group UV-absorbance is below 250 nm and coincides with the cut-off region of the many organic solvents, therefore the signal of a chiral guest is often used for interaction studies. One of the parameters that reflects chirality, the concentration independent value of the *g*-factor, is a good measure of chirality sensing. Inoue and Kim et al. [62] have shown that the *g*-factor of chiral charge transfer dyad **18** can be affected by complexation with CB[8] (Figure 17).

One step further from the creation of a chiral complex of CB through binding with a chiral guest is the compilation of a ternary system that can show stereoselectivity. The very first and very comprehensive study in this direction was done by the group of Inoue and Kim [63]. They investigated a number of ternary systems and found that the CB[6] complex with (*R*)-2-methylpiperazine is especially selective toward complexation with (*S*)-2-methylbutylamine ( $K = 15,000 \pm 3000 \text{ M}^{-1}$ )

if compared with the complex between (S)-2-methylpiperazine with (S)-2-methylbutylamine ( $K = 800 \pm 100 \text{ M}^{-1}$ ) (Figure 18). A matched enantiomer is bound with 19-times greater affinity than the mismatched enantiomer. It was claimed to be the highest enantioselectivity ever reported for a supramolecular system derived from an achiral host. To explain such a selectivity, an analogy to the commander-sergeant-soldier [64] system was exploited. Binding to CBs is governed by the hydrophobic effect related to the guest's ability to enter the CBs' cavity. Double-charged methylpiperazine is designated as a soldier, and it is weakly bound to CB at portals; it cannot enter the cavity, but can attract two CBs, causing aggregation of the CB-methylpiperazine complex. Aggregation can be minimized at a concentration below 0.3 mM. CB is designated as the sergeant, and its role is to mediate the formation of diastereomeric complexes between two ammonium compounds. 2-Methylbutylamine is the commander, as its binding controls the formation of the final complex. The mismatching enantiomer of 2-methylbutylamine induces an unfavorable change of enthalpy, leading to an endothermic reaction, which is explained by the unfavorable change in the geometry of the bound methylpiperazine. The matching enantiomer of 2-methylbutylamine, on the other hand, does not disturb the complex between CB and bound methylpiperazine and is therefore overall strongly favored, and its binding leads eventually to disaggregation of the CB complex. In addition, in this work, selectivity toward diastereomeric dipeptides was shown [63].

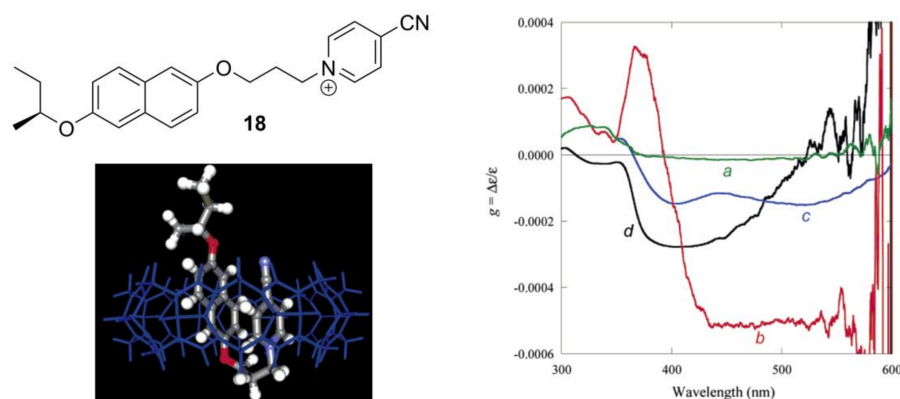


**Figure 17.** Structure of the charge-transfer dyad **18**; **18**@CB[8] complex 3D model and g-factor graph for: (a) the folded monomer in acetonitrile at 25 °C; (b) the head-to-tail dimer of **18** in  $\text{CH}_2\text{Cl}_2$  at  $-95$  °C; (c) the folded conformation in CB[8] in  $\text{D}_2\text{O}$  at 25 °C; (d) the inclusion complex with  $\alpha$ -CD in  $\text{H}_2\text{O}$  at 25 °C. Reprinted from [62].

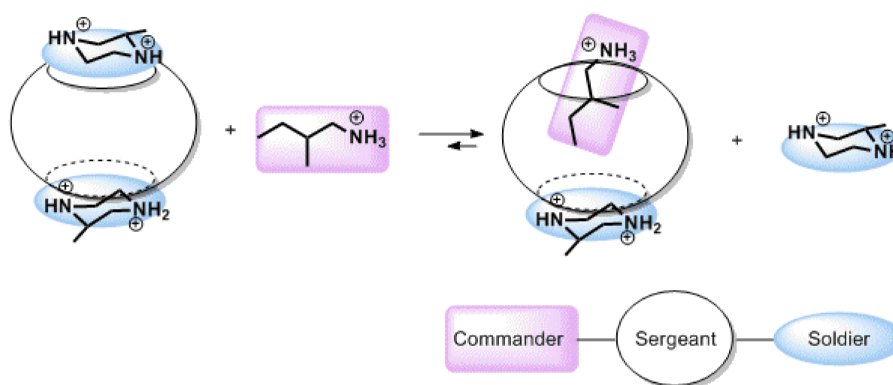


**Figure 18.** Representation of the complexation pathway in a ternary supramolecular system of CB[6], (S)-2-methylpiperazine and 2-methylbutylamine, with outstanding chiral selectivity [63].

The most recent study on a ternary system with two chiral compounds and CB[7] was published by Day et al. [65]. They observed that chiroptical properties of chiral organic salts can be affected by the formation of CB complexes. The most illustrative example of the effect of CB[7] is the change in the CD signal of diastereomeric pairs of chiral (*S*)-ammonium-2-benzyloxycyclopentane (*R*- or *S*-ABC<sup>+</sup>) salts with hydrogen tartrate (*L*- or *D*-HT<sup>−</sup>) (Figure 15). The additional absorption band is induced in the signal of one diastereomer (*S*-ABC@CB7·*D*-HT, the positive CD signal), as the other diastereomer signal retains the same  $\lambda_{\max}$  (*S*-ABC@CB7·*L*-HT, negative CD band) (Figure 19A). CB[7] has the same influence with respect to enantiomeric ammonium tartrate salts, and the sign of the Cotton effect is dictated by the chiral salt itself and is opposite for the signal for the enantiomeric pairs (Figure 19B).

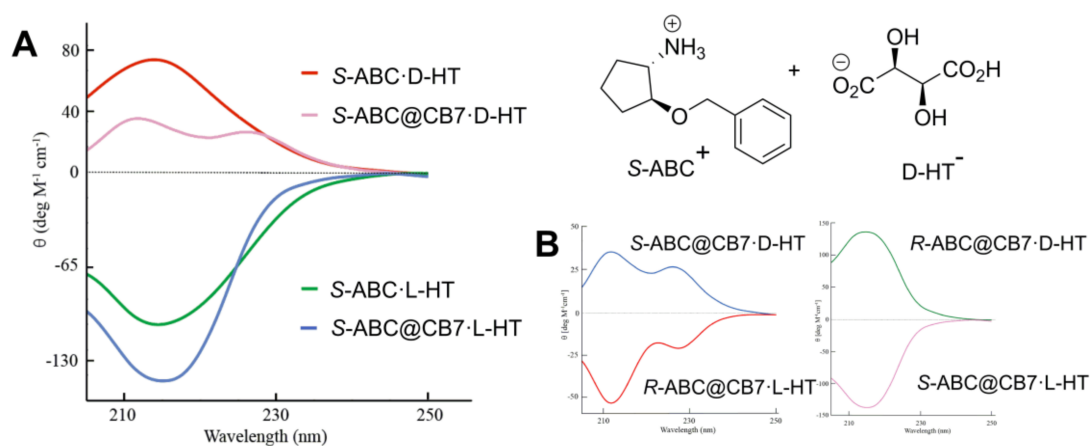


**Figure 19.** (A) CD signals for (*S*)-ammonium-2-benzyloxycyclopentane salt with *D*- and *L*-hydrogen tartrate and with and without CB[7]; (B) CD signal of two enantiomeric pairs of ternary complexes [65]. HT, hydrogen tartrate; (*S*)-ammonium-2-benzyloxycyclopentane (*S*-ABC<sup>+</sup>).

Based on the phenomena that chiral compounds can induce CD signal upon complexation with achiral molecules and that CB[8] forms a complex with two aromatic guests, Biedermann and Nau [66,67] developed a wonderful analytical method for the detection of chiral amino acids, peptides, proteins and aromatic drugs (Figure 20). Some examples of the application of this method are outlined in Figure 20B. One can follow the formation of some particular chiral product that chemoselectively forms a complex with a CB[8] sensor. In this sensor CB[8] acts as a host and fluorescent dye, for instance dimethyldiazaperopyrenium (MDPP), serves as a signaling unit. For example, during enzymatic hydrolysis of racemic glycyl-phenylalanine dipeptide (Gly-*D*/*L*-Phe), only one enantiomer is digested, and *L*-phenylalanine (*L*-Phe) is formed, while the Gly-*D*-Phe dipeptide remains intact. The binding constant of *L*-Phe ( $450 \times 10^3 \text{ M}^{-1}$ ) to supramolecular sensor MDPP@CB[8] is much higher, compared with binding of Gly-*D*-Phe ( $7 \times 10^3 \text{ M}^{-1}$ ) dipeptide; therefore, the [*L*-Phe·MDPP@CB[8]] complex is mainly formed, and *L*-Phe can be sensed through the CD signal of the ternary complex (Figure 20B, top). It is also remarkable that the kinetics of the enzyme reaction can be monitored by following the formation of a single enantiomer. Hippuryl-phenylalanine dipeptide hydrolysis kinetics, which was determined through the CD signal of the CB[8]-sensor system, coincides with conventionally measured UV-outcome, but in the first method, one can directly monitor enantioselectivity of the reaction and assign absolute configuration of the product.

In addition to chiral sensing applications, CBs have also been engaged in enantioselective supramolecular catalysis. Scherman and Herrmann et al. [68] showed that the CB[8] complex with a copper salt of a chiral amino acid can function as a chiral nanoreactor (Figure 21). The Diels-Alder reaction in the presence of CB[8], *L*-tryptophan and Cu<sup>2+</sup> gave cycloaddition product in enantiomeric excess (*ee*) of 73% compared with *ee* 31% from the reaction without CB. A catalytic system utilizing *N*- $\alpha$ -methyl-*L*-tryptophan as a chiral inducer gave the product in the presence of CB[8] in an *ee* of 92%

and without CB[8] in an *ee* of 72%. As a result, for the first time, it was shown that CB can increase enantioselectivity in the catalysis.

There are also fascinating examples of diastereoselective photocycloaddition reactions catalyzed by complexation with CBs, but as this topic has just been recently reviewed, it is not covered herein [28].

The presented examples show that there are outstanding approaches already proven to be possible, and noteworthy input has been made by studying complexation of chiral compounds with CBs. In addition to the examples described above, in Tables 1–4 is outlined a collection of chiral guests, whose complexation with CBs has been studied.

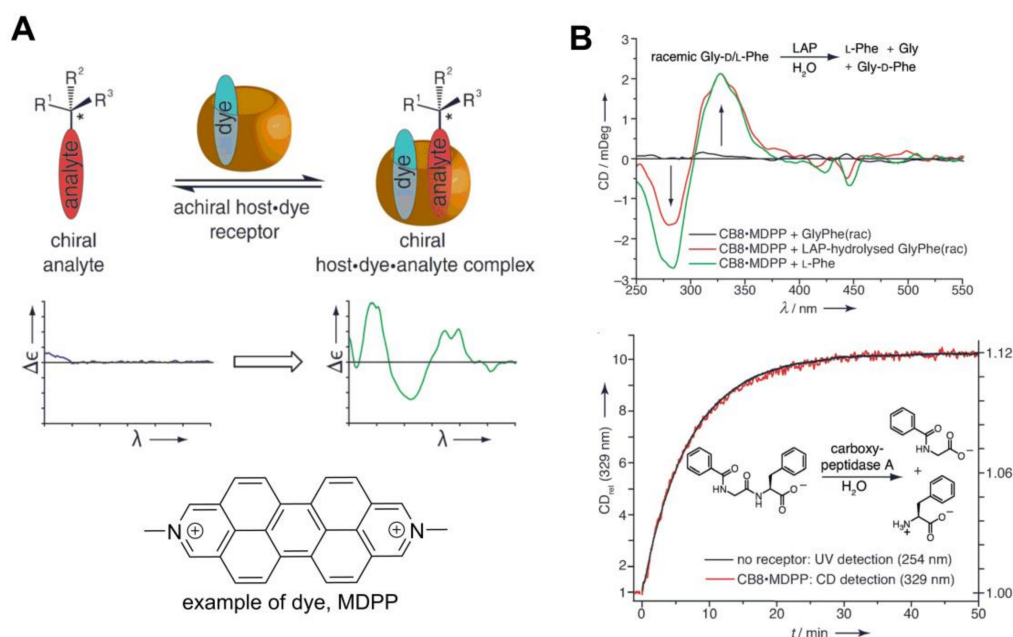


**Figure 20.** (A) Principle of the supramolecular chirality sensing system with CB[8]; (B) examples of the application of this sensing system: (top) CD spectra of CB[8]-MDPP (20 μM) in the presence of racemic Gly-D/L-Phe, before and after its enzymatic hydrolysis by leucine aminopeptidase (LAP) at pH 7.8; (bottom) kinetic trace for the hydrolysis of hippuryl-Phe (160 μM) by carboxypeptidase A at pH 7.8. The reaction progress was monitored by CD (329 nm) in the presence of MDPP@CB8 (20 μM, red line) and, as a control, directly by UV-Vis spectroscopy (254 nm, black line). Reprinted with permission from [66]. MDPP, dimethyldiazaperopyrenium.

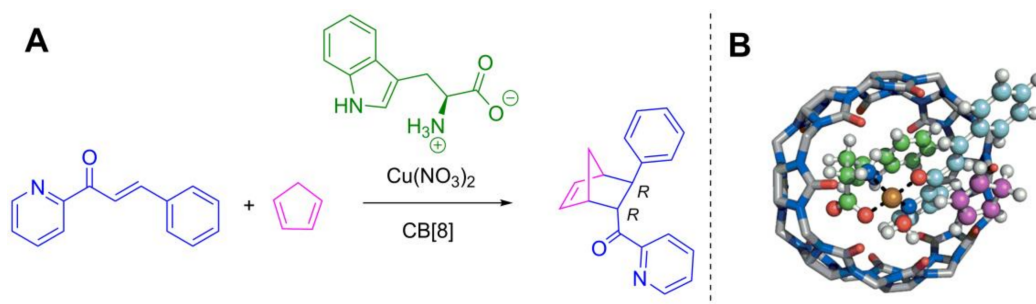


**Figure 21.** (A) Diels-Alder reaction catalyzed in a CB-nanoreactor; (B) lowest energy geometry of the complex of  $\text{Cu}^{2+}$ ,  $\text{H}_2\text{O}$ , tryptophan, azachalcone and CB[8] with cyclopentadiene approaching in the endo direction [68].

Table 1. Carbohydrates as guests for CBs (G, guest; H, Host; Ref, reference).

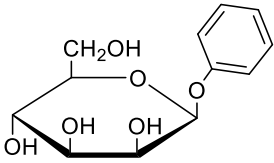
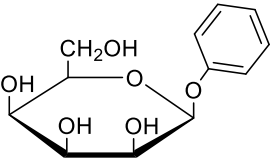
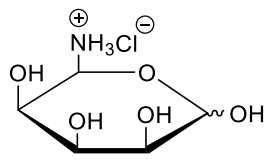
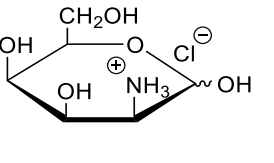
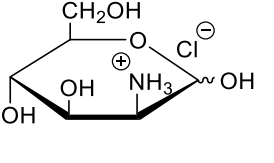
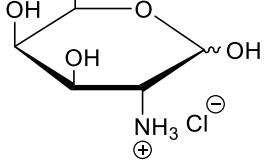
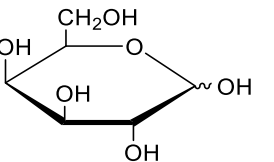
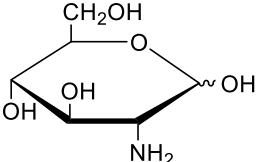
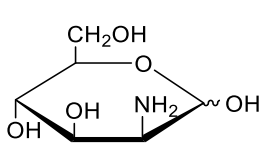
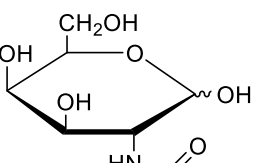
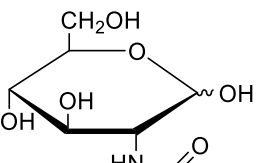
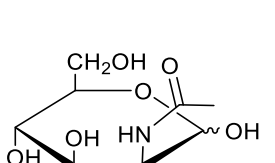
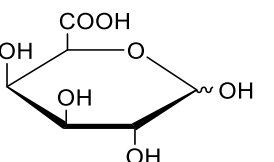
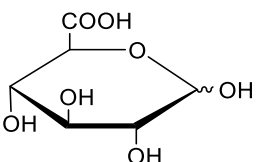
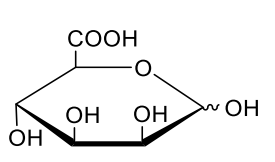
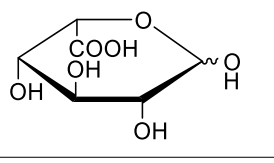
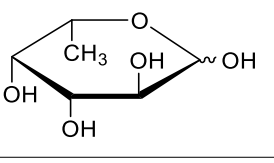
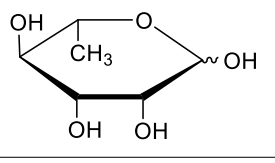
Legend	Structure of Guest, Name of Host and Reference Number		
G			
H	CB[8]	CB[8]	CB[7]
Ref.	[66]	[66]	[69]
G			
H		CB[7]	
Ref.		[69]	
G			
H		CB[7]	
Ref.		[70]	
G			
H		CB[7]	
Ref.		[70]	
G			
H		CB[7]	
Ref.		70	
G			
H		CB[7]	
Ref.		[70]	

Table 2. Pharmaceuticals as guests for CBs.

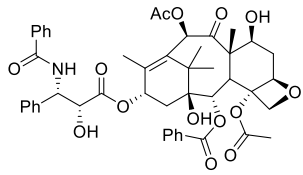
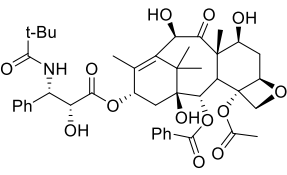
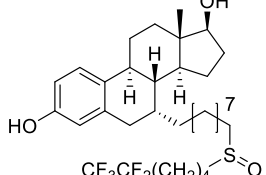
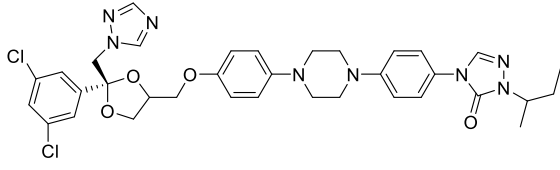
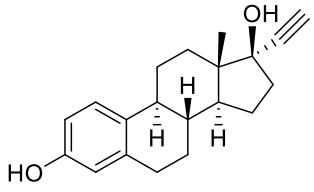
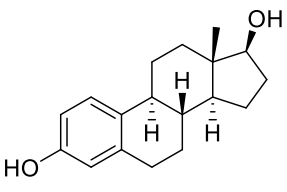
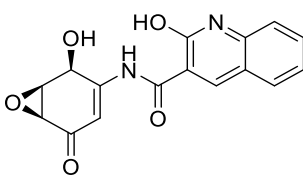
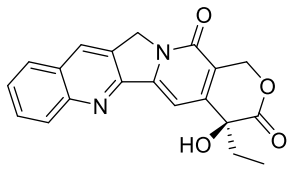
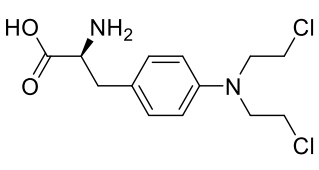
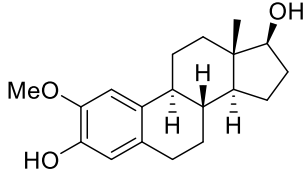
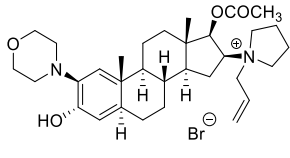
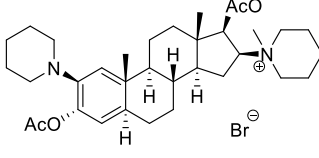
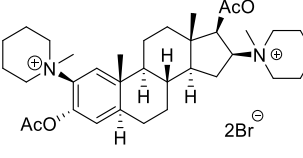
Legend	Structure of Guest, Name of Host and Reference Number		
G			
	Paclitaxel	Docetaxel	Fulvestrant
H	Acyclic CB		
Ref.	[71]		
G			
	Itraconazole	Voriconazole	
H	Acyclic CB		
Ref.	[71]		
G			
	$\alpha$ -ethynylestradiol	Estradiol	PBS 1086
H	Acyclic CB		
Ref.	[71–73]		
G			
	S-camptothecin	Melphalan	2-methoxyestradiol
H	Acyclic CB, CB[7], CB[8]	Acyclic CB	Acyclic CB
Ref.	[71–77]	[71–73]	[73]
G			
	Rocuronium	Vecuronium	Pancuronium
H	Acyclic CB		
Ref.	[78]		

Table 2. Cont.

Legend	Structure of Guest, Name of Host and Reference Number		
G			
	Cisatracurium		Tubocurarine
H	Acyclic CB		
Ref.	[78]		
G			
	Labetalol		Phenylephrine
H	CB[7]		CB[6], Acyclic CB
Ref.	[79]		[80]
G			
	Pseudoephedrine	Adrenaline	Amphetamine hydrochloride
H	CB[6], Acyclic CB	CB[6]	CB[7]
Ref.	[80]	[81]	[82]
G			
	Methamphetamine hydrochloride	Prilocaine	Sodium ascorbate
H	CB[7]	CB[7]	CB[6]
Ref.	[82]	[83]	[84]
G			
	Pilocarpine	6-monoacetylmorphine	Noroxycodone

Table 2. Cont.

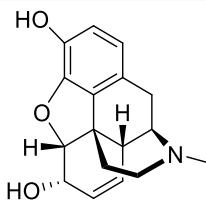
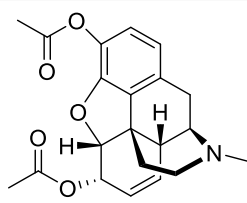
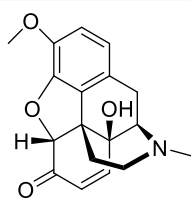
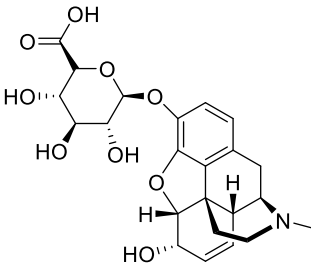
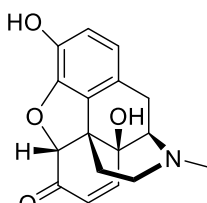
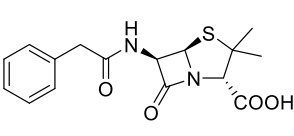
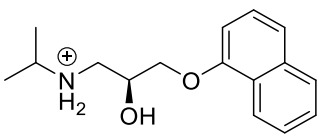
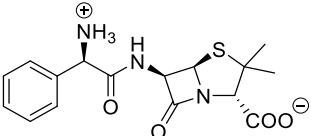
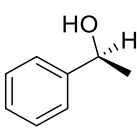
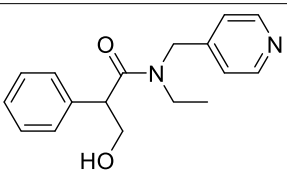
Legend	Structure of Guest, Name of Host and Reference Number		
H	CB[7]	Acyclic CB	Acyclic CB
Ref.	[85]	[86]	[86]
G			
	Morphine	Heroin	Oxycodone
H	Acyclic CB		
Ref.	[86]		
G			
	Normorphine	Morphine-6-glucuronide	Oxymorphone
H	Acyclic CB		
Ref.	[86]		
G			
	Penicillin G	(S)-propranolol	Ampicillin
H	CB[8]		
Ref.	[66]		
G			
	(S)-1-phenylethanol	Tropicamide	
H	CB[8]	CB[7], CB[8]	
Ref.	[66]	[87]	

Table 3. Amino acids, amino derivatives and peptides as guests for CBs.

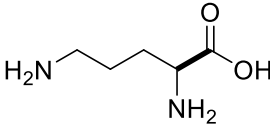
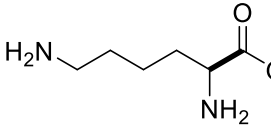
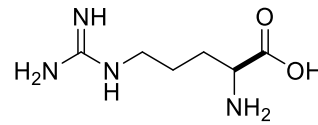
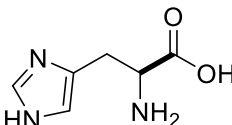
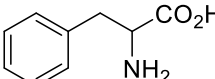
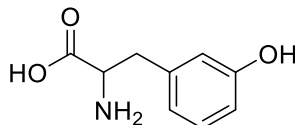
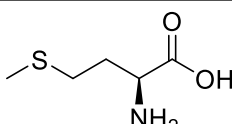
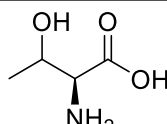
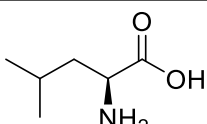
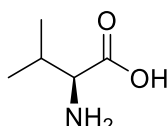
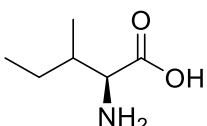
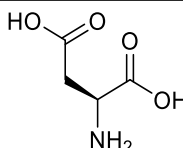
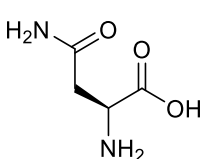
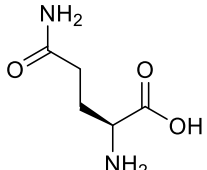
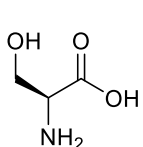
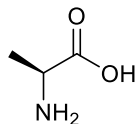
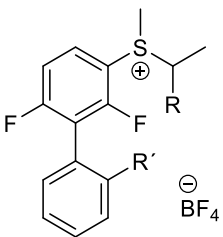
Legend	Structure of Guest, Name of Host and Reference Number		
G			
H	CB[6], Acyclic CB	CB[6], Acyclic, CB[7], iCB[7]	CB[6], Acyclic, CB[7], iCB[7]
Ref.	[88]	[82,89–92]	[82,89–92]
G			
H	CB[6], CB[7], CB[8], iCB[7]	CB[6], CB[7], CB[8], iCB[7]	CB[6], CB[7], CB[8], iCB[7]
Ref.	[82,89,91,93,94]	[89,91–96]	[89,92–94]
G			
H	iCB[7], CB[6]	iCB[7]	iCB[7]
Ref.	[91,97]	[91]	[91]
G			
H	iCB[7], CB[7]	iCB[7], CB[7]	CB[7]
Ref.	[91,92]	[91,92]	[92]
G			
H		CB[7]	
Ref.		[92]	
G			R = H, CH <sub>3</sub> ; R' = CH <sub>3</sub> , Cl
H	CB[7]	CB[8]	
Ref.	[92]	[98]	

Table 3. Cont.

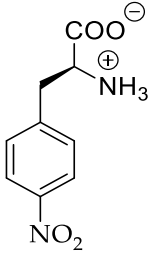
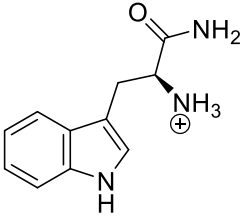
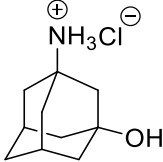
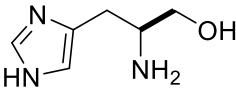
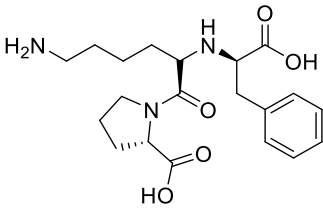
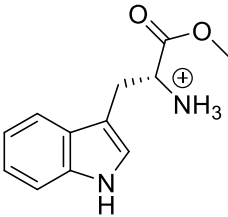
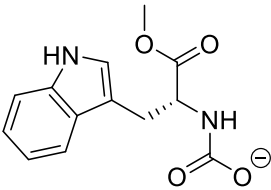
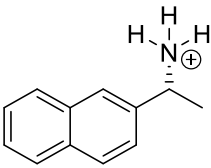
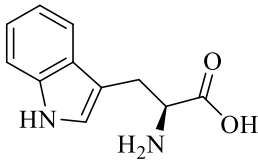
Legend	Structure of Guest, Name of Host and Reference Number		
G			
H	CB[7]		
Ref.	[66]		
G			
H	CB[6], Acyclic CB	CB[6], Acyclic CB	CB[8]
Ref.	[88]	[88]	[94]
G			
H	CB[8]	CB[7], CB[6]	CB[6], CB[8], iCB[7]
Ref.	[94]	[99]	[91,94,100,101]
G	Phe-Gly Phe-Ala Phe-Val Gly-Ala Asp-Phe Hippuryl-Phe	TrpPro Trp-OMe NAc-Trp Aspartame NAcTrp-NH2 Trp(Pro)6-NH2 Trp(Gly)6-NH2	Trp(Ala)6-NH2 Trp(Val)6-NH2 Trp(Leu)6-NH2 Trp(Asp)6-NH2 Trp(Glu)6-NH2 5-F-Trp(Gly)6-NH2 5-F-Trp(Asn)6-NH2
H	CB[8]		
Ref.	[66]		
G	Phe-Gly-Gly Gly-Phe-Gly Gly-Gly-Phe Gly-Gly-Trp-Gly-Gly	His-Gly-Gly Gly-His-Gly Gly-Gly-His Gly-Gly-Tyr Tyr-Gly-Gly	Gly-Tyr Gly-Trp Gly-Gly
H	CB[8]	CB[8]	CB[6]
Ref.	[102]	[102]	[103]
G	Gly-Tyr-Gly	Trp-Gly-Gly	Gly-Gly-Trp
H	CB[8]	CB[8]	CB[8]
Ref.	[102,104]	[94,102,104]	[94,102]

Table 3. Cont.

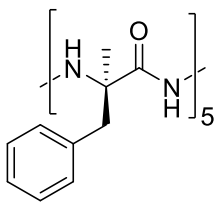
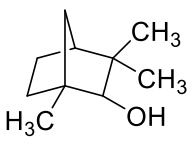
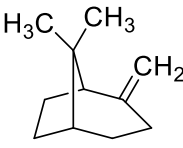
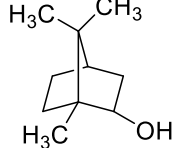
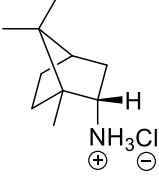
Legend	Structure of Guest, Name of Host and Reference Number		
G		Thr-Gly-Ala-Phe-Met Thr-Gly-Ala-AMPhe-Met	Phe-Leu Phe-Met-NH <sub>2</sub> Phe-Leu-NH <sub>2</sub> Thr-Gly-Ala-Phe-Leu Thr-Gly-Ala-Phe-Met-NH <sub>2</sub> Thr-Gly-Ala-Phe-Leu-NH <sub>2</sub> Thr-Gly-Ser-Phe-Met-NH <sub>2</sub> Thr-Gly-Gly-Phe-Met-NH <sub>2</sub> Thr-Gly-DAla-Phe-Met-NH <sub>2</sub>
H	CB[8]	CB[7]	CB[7]
Ref.	[105]	[106]	[96]
G	Gly-Phe		
H	CB[8], CB[6]		
Ref.	[51,88]		

Table 4. Terpenes as guests for CBs.

Legend	Structure of Guest, Name of Host and Reference Number			
G				
H	CB[7], CB[8]	CB[7]	CB[7]	CB[7]
Ref.	[74,107]	[107]	[107]	[108]

## 5. Conclusions

Cucurbituril chemistry has undergone remarkable growth in recent years. Applications of CB-type hosts have gained considerable attention due to CBs' outstanding binding ability and influence on the optical signal of dyes. However, studies on chiral sensing have emerged just recently, even though the first results in studies on the influence of CBs on supramolecular chirality appeared more than a decade ago. One can see that CB-type hosts are rich in means of symmetry breaking, which leads to induction of chirality. In addition, the synthesis of some chiral and enantiopure CB-type hosts have been developed, though the utilization of the created chiral systems is still obscure. Outstanding examples for the induction of supramolecular chirality from achiral building blocks and for the formation of helices in the solid state have been shown. Further on, the first elegant applications of the phenomena that CBs do form complexes with chiral guests and can induce specific chiroptical and catalytic properties are available. In addition, there are examples of stereoselective binding between diastereomers and cis–trans isomers, the selectivity of which is driven by the confined space inside the cucurbiturils. Based on that, the foundation for the emergence of new supramolecular systems, whose selectivity can be directed by external stimuli and that can be applied for chirality sensing and enantioselective applications, exists and should be encouraged.

**Acknowledgments:** The authors thank Sandra Kaabel for fruitful discussion and illustrations. The writing of this paper was supported by the Estonian Ministry of Education and Research through Grant PUT692.

**Author Contributions:** Both authors contributed substantially to the work reported.

**Conflicts of Interest:** The authors declare no conflict of interest.

## References

1. Freeman, W.A.; Mock, W.L.; Shih, N.Y. Cucurbituril. *J. Am. Chem. Soc.* **1981**, *103*, 7367–7368. [[CrossRef](#)]
2. Flinn, A.; Hough, G.C.; Stoddart, J.F.; Williams, D.J. Decamethylcucurbit[5]uril. *Angew. Chem. Int. Ed.* **1992**, *31*, 1475–1477. [[CrossRef](#)]
3. Kim, J.; Jung, I.-S.; Kim, S.-Y.; Lee, E.; Kang, J.-K.; Sakamoto, S.; Yamaguchi, K.; Kim, K. New Cucurbituril Homologues: Syntheses, Isolation, Characterization, and X-ray Crystal Structures of Cucurbit[*n*]uril (*n* = 5, 7, and 8). *J. Am. Chem. Soc.* **2000**, *122*, 540–541. [[CrossRef](#)]
4. Day, A.; Arnold, A.P.; Blanch, R.J.; Snushall, B. Controlling Factors in the Synthesis of Cucurbituril and Its Homologues. *J. Org. Chem.* **2001**, *66*, 8094–8100. [[CrossRef](#)] [[PubMed](#)]
5. Aav, R.; Kaabel, S.; Fomitšenko, M. Cucurbiturils: Synthesis, Structures, Formation Mechanisms, and Nomenclature. In *Comprehensive Supramolecular Chemistry II*; Atwood, J.L., Ed.; Elsevier: Oxford, UK, 2017; Volume 3, pp. 203–220, ISBN 978-0-12-803199-5.
6. Lisbjerg, M.; Pittelkow, M. Hemicucurbit[*n*]urils. In *Comprehensive Supramolecular Chemistry II*; Atwood, J.L., Ed.; Elsevier: Oxford, UK, 2017; Volume 3, pp. 221–236, ISBN 978-0-12-803199-5.
7. Ganapati, S.; Isaacs, L. Acyclic Cucurbit[*n*]uril-type Receptors: Preparation, Molecular Recognition Properties and Biological Applications. *Isr. J. Chem.* **2018**, in print. [[CrossRef](#)]
8. Andersen, N.N.; Lisbjerg, M.; Eriksen, K.; Pittelkow, M. Hemicucurbit[*n*]urils and Their Derivatives—Synthesis and Applications. *Isr. J. Chem.* **2018**, in print. [[CrossRef](#)]
9. Masson, E.; Raeisi, M.; Kotturi, K. Kinetics Inside, Outside and Through Cucurbiturils. *Isr. J. Chem.* **2018**, in print. [[CrossRef](#)]
10. Ouari, O.; Bardelang, D. Nitroxide Radicals with Cucurbit[*n*]urils and Other Cavitands. *Isr. J. Chem.* **2018**, in print. [[CrossRef](#)]
11. Shen, J.; Dearden, D.V. Recent Progress in Gas Phase Cucurbit[*n*]uril Chemistry. *Isr. J. Chem.* **2018**, in print. [[CrossRef](#)]
12. Kaifer, A.E. Portal Effects on the Stability of Cucurbituril Complexes. *Isr. J. Chem.* **2018**, in print. [[CrossRef](#)]
13. Hou, C.; Zeng, X.; Gao, Y.; Qiao, S.; Zhang, X.; Xu, J.; Liu, J. Cucurbituril As A Versatile Tool to Tune the Functions of Proteins. *Isr. J. Chem.* **2018**, in print. [[CrossRef](#)]
14. Kaabel, S.; Aav, R. Templating Effects in the Dynamic Chemistry of Cucurbiturils and Hemicucurbiturils. *Isr. J. Chem.* **2018**, in print. [[CrossRef](#)]
15. Wiemann, M.; Jonkheijm, P. Stimuli-Responsive Cucurbit[*n*]uril-Mediated Host-Guest Complexes on Surfaces. *Isr. J. Chem.* **2018**, in print. [[CrossRef](#)]
16. Vícha, R.; Jelínková, K.; Rouchal, M. Cucurbit[*n*]urils-related Multitopic Supramolecular Components: Design, Properties, and Perspectives. *Isr. J. Chem.* **2018**, in print. [[CrossRef](#)]
17. Koc, A.; Tuncel, D. Supramolecular Assemblies of Cucurbiturils with Photoactive,  $\pi$ -conjugated Chromophores. *Isr. J. Chem.* **2018**, in print. [[CrossRef](#)]
18. Robinson-Duggon, J.; Pérez-Mora, F.; Dibona-Villanueva, L.; Fuentealba, D. Potential Applications of Cucurbit[*n*]urils Inclusion Complexes in Photodynamic Therapy. *Isr. J. Chem.* **2018**, in print. [[CrossRef](#)]
19. Barooah, N.; Khurana, R.; Bhasikuttan, A.C.; Mohanty, J. Stimuli-responsive Supra-biomolecular Nanoassemblies of Cucurbit[7]uril with Bovine Serum Albumin: Drug Delivery and Sensor Applications. *Isr. J. Chem.* **2018**. [[CrossRef](#)]
20. Macartney, D.H. Cucurbit[*n*]uril Host-Guest Complexes of Acids, Photoacids, and Super Photoacids. *Isr. J. Chem.* **2018**. [[CrossRef](#)]
21. Masson, E.; Ling, X.; Joseph, R.; Kyeremeh-Mensah, L.; Lu, X. Cucurbituril chemistry: A tale of supramolecular success. *RSC Adv.* **2012**, *2*, 1213–1247. [[CrossRef](#)]
22. Tomas, L.; Vladimir, S. Bambusuril Anion Receptors. *Isr. J. Chem.* **2018**, in print. [[CrossRef](#)]
23. Reany, O.; Amar, M.; Ehud, K. Hetero-Bambusurils. *Isr. J. Chem.* **2018**, in print. [[CrossRef](#)]
24. Barrow, S.J.; Kaser, S.; Rowland, M.J.; del Barrio, J.; Scherman, O.A. Cucurbituril-Based Molecular Recognition. *Chem. Rev.* **2015**, *115*, 12320–12406. [[CrossRef](#)] [[PubMed](#)]
25. Sinn, S.; Biedermann, F. Chemical Sensors Based on Cucurbit[*n*]uril Macrocycles. *Isr. J. Chem.* **2018**, *58*. [[CrossRef](#)]
26. Ni, X.-L.; Xiao, X.; Cong, H.; Liang, L.-L.; Cheng, K.; Cheng, X.-J.; Ji, N.-N.; Zhu, Q.-J.; Xue, S.-F.; Tao, Z. Cucurbit[*n*]uril-based coordination chemistry: From simple coordination complexes to novel poly-dimensional coordination polymers. *Chem. Soc. Rev.* **2013**, *42*, 9480–9508. [[CrossRef](#)] [[PubMed](#)]

27. Ni, X.-L.; Xiao, X.; Cong, H.; Zhu, Q.-J.; Xue, S.-F.; Tao, Z. Self-Assemblies Based on the “Outer-Surface Interactions” of Cucurbit[n]urils: New Opportunities for Supramolecular Architectures and Materials. *Acc. Chem. Res.* **2014**, *47*, 1386–1395. [[CrossRef](#)] [[PubMed](#)]
28. Pattabiraman, M.; Sivaguru, J.; Ramamurthy, V. Cucurbiturils as Reaction Containers for Photocycloaddition of Olefins. *Isr. J. Chem.* **2017**, *57*, in print. [[CrossRef](#)]
29. Mandadapu, V.; Day, A.I.; Ghanem, A. Cucurbituril: Chiral Applications. *Chirality* **2014**, *26*, 712–723. [[CrossRef](#)] [[PubMed](#)]
30. Huang, W.-H.; Zavalij, P.Y.; Isaacs, L. Chiral Recognition inside a Chiral Cucurbituril. *Angew. Chem. Int. Ed.* **2007**, *46*, 7425–7427. [[CrossRef](#)] [[PubMed](#)]
31. Kozerski, L.; Hansen, P.E. Aggregation of amphiphilic molecules in water. I.  $\alpha$ -phenylethylamine:  $^1\text{H}$  and  $^{13}\text{C}$  NMR study. *J. Phys. Org. Chem.* **1991**, *4*, 58–66. [[CrossRef](#)]
32. Parve, O.; Reile, I.; Parve, J.; Kasvandik, S.; Kudrjašova, M.; Tamp, S.; Metsala, A.; Villo, L.; Pehk, T.; Jarvet, J.; et al. An NMR and MD Modeling Insight into Nucleation of 1,2-Alkanediols: Selective Crystallization of Lipase-Catalytically Resolved Enantiomers from the Reaction Mixtures. *J. Org. Chem.* **2013**, *78*, 12795–12801. [[CrossRef](#)] [[PubMed](#)]
33. Huang, W.-H.; Zavalij, P.Y.; Isaacs, L. Metal-Ion-Induced Folding and Dimerization of a Glycoluril Decamer in Water. *Org. Lett.* **2009**, *11*, 3918–3921. [[CrossRef](#)] [[PubMed](#)]
34. Cheng, X.-J.; Liang, L.-L.; Chen, K.; Ji, N.-N.; Xiao, X.; Zhang, J.-X.; Zhang, Y.-Q.; Xue, S.-F.; Zhu, Q.-J.; Ni, X.-L.; et al. Twisted Cucurbit[14]uril. *Angew. Chem. Int. Ed.* **2013**, *52*, 7252–7255. [[CrossRef](#)] [[PubMed](#)]
35. Qiu, S.-C.; Chen, K.; Wang, Y.; Hua, Z.; Li, F.; Huang, Y.; Tao, Z.; Zhang, Y.; Wei, G. Crystal structure analysis of twisted cucurbit [14]uril conformations. *Inorg. Chem. Commun.* **2017**, *86*, 49–53. [[CrossRef](#)]
36. Li, Q.; Qiu, S.-C.; Zhang, J.; Chen, K.; Huang, Y.; Xiao, X.; Zhang, Y.; Li, F.; Zhang, Y.-Q.; Xue, S.-F.; et al. Twisted Cucurbit[n]urils. *Org. Lett.* **2016**, *18*, 4020–4023. [[CrossRef](#)] [[PubMed](#)]
37. Lu, X.; Isaacs, L. Synthesis and Recognition Properties of Enantiomerically Pure Acyclic Cucurbit[n]uril-Type Molecular Containers. *Org. Lett.* **2015**, *17*, 4038–4041. [[CrossRef](#)] [[PubMed](#)]
38. Cao, L.; Hettiarachchi, G.; Briken, V.; Isaacs, L. Cucurbit[7]uril Containers for Targeted Delivery of Oxaliplatin to Cancer Cells. *Angew. Chem. Int. Ed.* **2013**, *52*, 12033–12037. [[CrossRef](#)] [[PubMed](#)]
39. Chen, J.; Liu, Y.; Mao, D.; Ma, D. Acyclic cucurbit[n]uril conjugated dextran for drug encapsulation and bioimaging. *Chem. Commun.* **2017**, *53*, 8739–8742. [[CrossRef](#)] [[PubMed](#)]
40. Herges, R. Topology in Chemistry: Designing Möbius Molecules. *Chem. Rev.* **2006**, *106*, 4820–4842. [[CrossRef](#)] [[PubMed](#)]
41. Li, Q.; Qiu, S.-C.; Chen, K.; Zhang, Y.; Wang, R.; Huang, Y.; Tao, Z.; Zhu, Q.-J.; Liu, J.-X. Encapsulation of alkylidiammonium ions within two different cavities of twisted cucurbit[14]uril. *Chem. Commun.* **2016**, *52*, 2589–2592. [[CrossRef](#)] [[PubMed](#)]
42. Miyahara, Y.; Goto, K.; Oka, M.; Inazu, T. Remarkably Facile Ring-Size Control in Macrocyclization: Synthesis of Hemicucurbit[6]uril and Hemicucurbit[12]uril. *Angew. Chem. Int. Ed.* **2004**, *43*, 5019–5022. [[CrossRef](#)] [[PubMed](#)]
43. Svec, J.; Necas, M.; Sindelar, V. Bambus[6]uril. *Angew. Chem. Int. Ed.* **2010**, *49*, 2378–2381. [[CrossRef](#)] [[PubMed](#)]
44. Singh, M.; Solel, E.; Keinan, E.; Reany, O. Aza-Bambusurils En Route to Anion Transporters. *Chem. Eur. J.* **2016**, *22*, 8848–8854. [[CrossRef](#)] [[PubMed](#)]
45. Aav, R.; Shmatova, E.; Reile, I.; Borissova, M.; Topić, F.; Rissanen, K. New Chiral Cyclohexylhemicucurbit[6]uril. *Org. Lett.* **2013**, *15*, 3786–3789. [[CrossRef](#)] [[PubMed](#)]
46. Lisbjerg, M.; Jessen, B.M.; Rasmussen, B.; Nielsen, B.E.; Madsen, A.Ø.; Pittelkow, M. Discovery of a cyclic 6 + 6 hexamer of D-biotin and formaldehyde. *Chem. Sci.* **2014**, *5*, 2647–2650. [[CrossRef](#)]
47. Prigorchenko, E.; Öeren, M.; Kaabel, S.; Fomitšenko, M.; Reile, I.; Järving, I.; Tamm, T.; Topić, F.; Rissanen, K.; Aav, R. Template-controlled synthesis of chiral cyclohexylhemicucurbit[8]uril. *Chem. Commun.* **2015**, *51*, 10921–10924. [[CrossRef](#)] [[PubMed](#)]
48. Öeren, M.; Shmatova, E.; Tamm, T.; Aav, R. Computational and ion mobility MS study of (all-S)-cyclohexylhemicucurbit[6]uril structure and complexes. *Phys. Chem. Chem. Phys.* **2014**, *16*, 19198–19205. [[CrossRef](#)] [[PubMed](#)]
49. Kaabel, S.; Adamson, J.; Topić, F.; Kiesilä, A.; Kalenius, E.; Öeren, M.; Reimund, M.; Prigorchenko, E.; Löökene, A.; Reich, H.J.; et al. Chiral hemicucurbit[8]uril as an anion receptor: Selectivity to size, shape and charge distribution. *Chem. Sci.* **2017**, *8*, 2184–2190. [[CrossRef](#)] [[PubMed](#)]

50. Lisbjerg, M.; Nielsen, B.E.; Milhøj, B.O.; Sauer, S.P.A.; Pittelkow, M. Anion binding by biotin[6]uril in water. *Org. Biomol. Chem.* **2014**, *13*, 369–373. [[CrossRef](#)] [[PubMed](#)]
51. Lisbjerg, M.; Valkenier, H.; Jessen, B.M.; Al-Kerdi, H.; Davis, A.P.; Pittelkow, M. Biotin[6]uril Esters: Chloride-Selective Transmembrane Anion Carriers Employing C–H···Anion Interactions. *J. Am. Chem. Soc.* **2015**, *137*, 4948–4951. [[CrossRef](#)] [[PubMed](#)]
52. Leong, W.L.; Vittal, J.J. One-Dimensional Coordination Polymers: Complexity and Diversity in Structures, Properties, and Applications. *Chem. Rev.* **2011**, *111*, 688–764. [[CrossRef](#)] [[PubMed](#)]
53. Whang, D.; Kim, K. Helical polyrotaxane: Cucurbituril ‘beads’ threaded onto a helical one-dimensional coordination polymer. *Chem. Commun.* **1997**, 2361–2362. [[CrossRef](#)]
54. Park, K.-M.; Whang, D.; Lee, E.; Heo, J.; Kim, K. Transition Metal Ion Directed Supramolecular Assembly of One- and Two-Dimensional Polyrotaxanes Incorporating Cucurbituril. *Chem. Eur. J.* **2002**, *8*, 498–508. [[CrossRef](#)]
55. Zeng, J.-P.; Cong, H.; Chen, K.; Xue, S.-F.; Zhang, Y.-Q.; Zhu, Q.-J.; Liu, J.-X.; Tao, Z. A Novel Strategy to Assemble Achiral Ligands to Chiral Helical Polyrotaxane Structures. *Inorg. Chem.* **2011**, *50*, 6521–6525. [[CrossRef](#)] [[PubMed](#)]
56. Zhang, F.; Yajima, T.; Li, Y.-Z.; Xu, G.-Z.; Chen, H.-L.; Liu, Q.-T.; Yamauchi, O. Iodine-Assisted Assembly of Helical Coordination Polymers of Cucurbituril and Asymmetric Copper(II) Complexes. *Angew. Chem. Int. Ed.* **2005**, *44*, 3402–3407. [[CrossRef](#)] [[PubMed](#)]
57. Chen, K.; Hu, Y.-F.; Xiao, X.; Xue, S.-F.; Tao, Z.; Zhang, Y.-Q.; Zhu, Q.-J.; Liu, J.-X. Homochiral 1D-helical coordination polymers from achiral cucurbit[5]uril: Hydroquinone-induced spontaneous resolution. *RSC Adv.* **2012**, *2*, 3217–3220. [[CrossRef](#)]
58. Chen, K.; Liang, L.-L.; Liu, H.-J.; Zhang, Y.-Q.; Xue, S.-F.; Tao, Z.; Xiao, X.; Zhu, Q.-J.; Lindoy, L.F.; Wei, G. Hydroquinone-assisted assembly of coordination polymers from lanthanides and cucurbit[5]uril. *CrystEngComm* **2012**, *14*, 7994–7999. [[CrossRef](#)]
59. Xiao, X.; Liu, J.-X.; Fan, Z.-F.; Chen, K.; Zhu, Q.-J.; Xue, S.-F.; Tao, Z. Chirality from achiral components: *N,N'*-bis(4-dimethylaminobenzyl)dodecane-1,12-diammonium in cucurbit[8]uril. *Chem. Commun.* **2010**, *46*, 3741–3743. [[CrossRef](#)] [[PubMed](#)]
60. Hembury, G.A.; Borovkov, V.V.; Inoue, Y. Chirality-Sensing Supramolecular Systems. *Chem. Rev.* **2008**, *108*, 1–73. [[CrossRef](#)] [[PubMed](#)]
61. Liu, M.; Zhang, L.; Wang, T. Supramolecular Chirality in Self-Assembled Systems. *Chem. Rev.* **2015**, *115*, 7304–7397. [[CrossRef](#)] [[PubMed](#)]
62. Mori, T.; Ko, Y.H.; Kim, K.; Inoue, Y. Circular Dichroism of Intra- and Intermolecular Charge-Transfer Complexes. Enhancement of Anisotropy Factors by Dimer Formation and by Confinement. *J. Org. Chem.* **2006**, *71*, 3232–3247. [[CrossRef](#)] [[PubMed](#)]
63. Rekharsky, M.V.; Yamamura, H.; Inoue, C.; Kawai, M.; Osaka, I.; Arakawa, R.; Shiba, K.; Sato, A.; Ko, Y.H.; Selvapalam, N.; et al. Chiral Recognition in Cucurbituril Cavities. *J. Am. Chem. Soc.* **2006**, *128*, 14871–14880. [[CrossRef](#)] [[PubMed](#)]
64. Green, M.M.; Reidy, M.P.; Johnson, R.D.; Darling, G.; O’Leary, D.J.; Willson, G. Macromolecular stereochemistry: The out-of-proportion influence of optically active comonomers on the conformational characteristics of polyisocyanates. The sergeants and soldiers experiment. *J. Am. Chem. Soc.* **1989**, *111*, 6452–6454. [[CrossRef](#)]
65. Wu, W.; Cronin, M.P.; Wallace, L.; Day, A.I. An Exploration of Induced Supramolecular Chirality Through Association of Chiral Ammonium Ions and Tartrates with the Achiral Host Cucurbit[7]uril. *Isr. J. Chem.* **2018**, *58*, in print. [[CrossRef](#)]
66. Biedermann, F.; Nau, W.M. Noncovalent Chirality Sensing Ensembles for the Detection and Reaction Monitoring of Amino Acids, Peptides, Proteins, and Aromatic Drugs. *Angew. Chem. Int. Ed.* **2014**, *53*, 5694–5699. [[CrossRef](#)] [[PubMed](#)]
67. Nau, W.; Biedermann, F. A Method for Detecting a Chiral Analyte. Patent DE102013021899A1, 2015. Available online: <https://patents.google.com/patent/DE102013021899A1/en> (accessed on 2 February 2018).
68. Zheng, L.; Sonzini, S.; Ambarwati, M.; Rosta, E.; Scherman, O.A.; Herrmann, A. Turning Cucurbit[8]uril into a Supramolecular Nanoreactor for Asymmetric Catalysis. *Angew. Chem. Int. Ed.* **2015**, *54*, 13007–13011. [[CrossRef](#)] [[PubMed](#)]

69. Jang, Y.; Natarajan, R.; Ko, Y.H.; Kim, K. Cucurbit[7]uril: A High-Affinity Host for Encapsulation of Amino Saccharides and Supramolecular Stabilization of Their  $\alpha$ -Anomers in Water. *Angew. Chem. Int. Ed.* **2014**, *53*, 1003–1007. [[CrossRef](#)] [[PubMed](#)]
70. Lee, H.H.L.; Kim, H.I. Supramolecular Analysis of Monosaccharide Derivatives Using Cucurbit[7]uril and Electrospray Ionization Tandem Mass Spectrometry. *Isr. J. Chem.* **2018**, in print. [[CrossRef](#)]
71. Zhang, B.; Isaacs, L. Acyclic Cucurbit[n]uril-type Molecular Containers: Influence of Aromatic Walls on their Function as Solubilizing Excipients for Insoluble Drugs. *J. Med. Chem.* **2014**, *57*, 9554–9563. [[CrossRef](#)] [[PubMed](#)]
72. Gilberg, L.; Zhang, B.; Zavalij, P.Y.; Sindelar, V.; Isaacs, L. Acyclic cucurbit[n]uril-type molecular containers: Influence of glycoluril oligomer length on their function as solubilizing agents. *Org. Biomol. Chem.* **2015**, *13*, 4041–4050. [[CrossRef](#)] [[PubMed](#)]
73. Sigwalt, D.; Moncelet, D.; Falcinelli, S.; Mandadapu, V.; Zavalij, P.Y.; Day, A.; Briken, V.; Isaacs, L. Acyclic Cucurbit[n]uril-Type Molecular Containers: Influence of Linker Length on Their Function as Solubilizing Agents. *ChemMedChem* **2016**, *11*, 980–989. [[CrossRef](#)] [[PubMed](#)]
74. Romero, M.A.; González-Delgado, J.A.; Mendoza, J.; Arteaga, J.F.; Basilio, N.; Pischel, U. Terpenes Show Nanomolar Affinity and Selective Binding with Cucurbit[8]uril. *Isr. J. Chem.* **2018**, in print. [[CrossRef](#)]
75. Gavvala, K.; Sengupta, A.; Hazra, P. Modulation of Photophysics and pKa Shift of the Anti-cancer Drug Camptothecin in the Nanocavities of Supramolecular Hosts. *ChemPhysChem* **2013**, *14*, 532–542. [[CrossRef](#)] [[PubMed](#)]
76. Dong, N.; Xue, S.-F.; Zhu, Q.-J.; Tao, Z.; Zhao, Y.; Yang, L.-X. Cucurbit[n]urils ( $n = 7, 8$ ) binding of camptothecin and the effects on solubility and reactivity of the anticancer drug. *Supramol. Chem.* **2008**, *20*, 663–671. [[CrossRef](#)]
77. Yang, X.; Wang, Z.; Niu, Y.; Chen, X.; Lee, S.M.Y.; Wang, R. Influence of supramolecular encapsulation of camptothecin by cucurbit[7]uril: Reduced toxicity and preserved anti-cancer activity. *Med. Chem. Comm.* **2016**, *7*, 1392–1397. [[CrossRef](#)]
78. Ma, D.; Zhang, B.; Hoffmann, U.; Sundrup, M.G.; Eikermann, M.; Isaacs, L. Acyclic Cucurbit[n]uril-Type Molecular Containers Bind Neuromuscular Blocking Agents In Vitro and Reverse Neuromuscular Block In Vivo. *Angew. Chem. Int. Ed.* **2012**, *51*, 11358–11362. [[CrossRef](#)] [[PubMed](#)]
79. Li, C.; Feng, J.; Ju, H. Supramolecular interaction of labelalol with cucurbit[7]uril for its sensitive fluorescence detection. *Analyst* **2014**, *140*, 230–235. [[CrossRef](#)] [[PubMed](#)]
80. Minami, T.; Esipenko, N.A.; Akdeniz, A.; Zhang, B.; Isaacs, L.; Anzenbacher, P. Multianalyte Sensing of Addictive Over-the-Counter (OTC) Drugs. *J. Am. Chem. Soc.* **2013**, *135*, 15238–15243. [[CrossRef](#)] [[PubMed](#)]
81. Danylyuk, O.; Fedin, V.P.; Sashuk, V. Kinetic trapping of the host–guest association intermediate and its transformation into a thermodynamic inclusion complex. *Chem. Commun.* **2013**, *49*, 1859–1861. [[CrossRef](#)] [[PubMed](#)]
82. Jang, Y.; Jang, M.; Kim, H.; Lee, S.J.; Jin, E.; Koo, J.Y.; Hwang, I.-C.; Kim, Y.; Ko, Y.H.; Hwang, I.; et al. Point-of-Use Detection of Amphetamine-Type Stimulants with Host-Molecule-Functionalized Organic Transistors. *Chem* **2017**, *3*, 641–651. [[CrossRef](#)]
83. Wyman, I.W.; Macartney, D.H. Host–guest complexations of local anaesthetics by cucurbit[7]uril in aqueous solution. *Org. Biomol. Chem.* **2010**, *8*, 247–252. [[CrossRef](#)] [[PubMed](#)]
84. Pandey, S.; Soni, V.K.; Choudhary, G.; Sharma, P.R.; Sharma, R.K. Understanding behaviour of vitamin-C guest binding with the cucurbit[6]uril host. *Supramol. Chem.* **2017**, *29*, 387–394. [[CrossRef](#)]
85. Saleh, N.; Al-Handawi, M.B.; Al-Kaabi, L.; Ali, L.; Salman Ashraf, S.; Thiemann, T.; al-Hindawi, B.; Meetani, M. Intermolecular interactions between cucurbit[7]uril and pilocarpine. *Int. J. Pharm.* **2014**, *460*, 53–62. [[CrossRef](#)] [[PubMed](#)]
86. Shcherbakova, E.G.; Zhang, B.; Gozem, S.; Minami, T.; Zavalij, P.Y.; Pushina, M.; Isaacs, L.D.; Anzenbacher, P. Supramolecular Sensors for Opiates and Their Metabolites. *J. Am. Chem. Soc.* **2017**, *139*, 14954–14960. [[CrossRef](#)] [[PubMed](#)]
87. Saleh, N.; Meetani, M.A.; Al-Kaabi, L.; Ghosh, I.; Nau, W.M. Effect of cucurbit[n]urils on tropicamide and potential application in ocular drug delivery. *Supramol. Chem.* **2011**, *23*, 650–656. [[CrossRef](#)]
88. Minami, T.; Esipenko, N.A.; Zhang, B.; Isaacs, L.; Anzenbacher, P. “Turn-on” fluorescent sensor array for basic amino acids in water. *Chem. Commun.* **2014**, *50*, 61–63. [[CrossRef](#)] [[PubMed](#)]
89. Lee, J.W.; Lee, H.H.L.; Ko, Y.H.; Kim, K.; Kim, H.I. Deciphering the Specific High-Affinity Binding of Cucurbit[7]uril to Amino Acids in Water. *J. Phys. Chem. B* **2015**, *119*, 4628–4636. [[CrossRef](#)] [[PubMed](#)]

90. Bailey, D.M.; Hennig, A.; Uzunova, V.D.; Nau, W.M. Supramolecular Tandem Enzyme Assays for Multiparameter Sensor Arrays and Enantiomeric Excess Determination of Amino Acids. *Chem. Eur. J.* **2008**, *14*, 6069–6077. [[CrossRef](#)] [[PubMed](#)]
91. Gao, Z.-Z.; Kan, J.-L.; Chen, L.-X.; Bai, D.; Wang, H.-Y.; Tao, Z.; Xiao, X. Binding and Selectivity of Essential Amino Acid Guests to the Inverted Cucurbit[7]uril Host. *ACS Omega* **2017**, *2*, 5633–5640. [[CrossRef](#)]
92. Kovalenko, E.; Vilaseca, M.; Díaz-Lobo, M.; Masliy, A.N.; Vicent, C.; Fedin, V.P. Supramolecular Adducts of Cucurbit[7]uril and Amino Acids in the Gas Phase. *J. Am. Soc. Mass Spectrom.* **2016**, *27*, 265–276. [[CrossRef](#)] [[PubMed](#)]
93. Hang, C.; Tau, L.-L.; Yu, Y.-H.; Yang, F.; Du, Y.; Xue, S.-F.; Tao, Z. Molecular Recognition of Amino acid by Cucurbiturils. *Acta Chim. Sin.* **2006**, *64*, 989–996.
94. Bush, M.E.; Bouley, N.D.; Urbach, A.R. Charge-Mediated Recognition of N-Terminal Tryptophan in Aqueous Solution by a Synthetic Host. *J. Am. Chem. Soc.* **2005**, *127*, 14511–14517. [[CrossRef](#)] [[PubMed](#)]
95. Liu, S.; Ruspic, C.; Mukhopadhyay, P.; Chakrabarti, S.; Zavalij, P.Y.; Isaacs, L. The Cucurbit[n]uril Family: Prime Components for Self-Sorting Systems. *J. Am. Chem. Soc.* **2005**, *127*, 15959–15967. [[CrossRef](#)] [[PubMed](#)]
96. Ghale, G.; Ramalingam, V.; Urbach, A.R.; Nau, W.M. Determining Protease Substrate Selectivity and Inhibition by Label-Free Supramolecular Tandem Enzyme Assays. *J. Am. Chem. Soc.* **2011**, *133*, 7528–7535. [[CrossRef](#)] [[PubMed](#)]
97. Thuéry, P. Supramolecular assemblies built from lanthanide ammoniocarboxylates and cucurbit[6]uril. *CrystEngComm* **2012**, *14*, 8128–8136. [[CrossRef](#)]
98. Joseph, R.; Masson, E. Cucurbit[8]uril recognition of rapidly interconverting diastereomers. *Supramol. Chem.* **2014**, *26*, 632–641. [[CrossRef](#)]
99. Tang, H.; Fuentealba, D.; Ko, Y.H.; Selvapalam, N.; Kim, K.; Bohne, C. Guest Binding Dynamics with Cucurbit[7]uril in the Presence of Cations. *J. Am. Chem. Soc.* **2011**, *133*, 20623–20633. [[CrossRef](#)] [[PubMed](#)]
100. Danylyuk, O.; Fedin, V.P. Solid-State Supramolecular Assemblies of Tryptophan and Tryptamine with Cucurbit[6]uril. *Cryst. Growth Des.* **2012**, *12*, 550–555. [[CrossRef](#)]
101. Ling, Y.; Wang, W.; Kaifer, A.E. A new cucurbit[8]uril-based fluorescent receptor for indole derivatives. *Chem. Commun.* **2007**, 610–612. [[CrossRef](#)] [[PubMed](#)]
102. Heitmann, L.M.; Taylor, A.B.; Hart, P.J.; Urbach, A.R. Sequence-specific recognition and cooperative dimerization of n-terminal aromatic peptides in aqueous solution by a synthetic host. *J. Am. Chem. Soc.* **2006**, *128*, 12574–12581. [[CrossRef](#)] [[PubMed](#)]
103. Danylyuk, O. Exploring cucurbit[6]uril–peptide interactions in the solid state: Crystal structure of cucurbit[6]uril complexes with glycyl-containing dipeptides. *CrystEngComm* **2017**, *19*, 3892–3897. [[CrossRef](#)]
104. Biedermann, F.; Rauwald, U.; Cziferszky, M.; Williams, K.A.; Gann, L.D.; Guo, B.Y.; Urbach, A.R.; Bielawski, C.W.; Scherman, O.A. Benzobis(imidazolium)–Cucurbit[8]uril Complexes for Binding and Sensing Aromatic Compounds in Aqueous Solution. *Chem. Eur. J.* **2010**, *16*, 13716–13722. [[CrossRef](#)] [[PubMed](#)]
105. Sonzini, S.; Ryan, S.T.J.; Scherman, O.A. Supramolecular dimerisation of middle-chain Phe pentapeptides via CB[8] host–guest homoternary complex formation. *Chem. Commun.* **2013**, *49*, 8779–8781. [[CrossRef](#)] [[PubMed](#)]
106. Logsdon, L.A.; Urbach, A.R. Sequence-Specific Inhibition of a Nonspecific Protease. *J. Am. Chem. Soc.* **2013**, *135*, 11414–11416. [[CrossRef](#)] [[PubMed](#)]
107. Romero, M.A.; Basilio, N.; Moro, A.J.; Domingues, M.; González-Delgado, J.A.; Arteaga, J.F.; Pischel, U. Photocaged Competitor Guests: A General Approach Toward Light-Activated Cargo Release from Cucurbiturils. *Chem. Eur. J.* **2017**, *23*, 13105–13111. [[CrossRef](#)] [[PubMed](#)]
108. Cao, L.; Isaacs, L. Absolute and relative binding affinity of cucurbit[7]uril towards a series of cationic guests. *Supramol. Chem.* **2014**, *26*, 251–258. [[CrossRef](#)]

